ATTACHMENT 3

GLOBAL NUCLEAR FUEL - AMERICAS LLC

MCNP01A

LOW ENRICHED UO2 PIN LATTICE IN WATER CRITICAL BENCHMARK EVALUATIONS USING ENDF/B-V NUCLEAR CROSS-SECTION DATA, REVISION 1

(NON-PROPRIETARY)

Nine Mile Point Nuclear Station, LLC
July 30, 2010

Global Nuclear Fuel

A Joint Venture of GE, Toshiba, & Hitachi

0000-0032-0998-R2
eDRF: 0000-0032-0996 Rev.0
eDRF Section: 0000-0032-0998 Rev.1

Class I
June 2010

MCNP01A Low Enriched UO_2 Pin Lattice in Water Critical Benchmark Evaluations Using ENDF/B-V Nuclear Cross-Section Data

Revision 1

NON-PROPRIETARY NOTICE

This is a non-proprietary version of the document MCNP01A Low Enriched UO_2 Pin Lattice in Water Critical Benchmark Evaluations Using ENDF/B-V Nuclear Cross-Section Data Revision 1, from which the proprietary information has been removed. Portions of the document that have been removed are identified by white space within double square brackets, as shown here [[ ]].

IMPORTANT NOTICE REGARDING CONTENTS OF THIS REPORT

Please read carefully

The design, engineering, and other information contained in this document is furnished for the purpose of supporting submittal of NMP2 Extended Power Uprate as stated in the transmittal letter. The only undertakings of GNF with respect to information in this document are contained in the contracts between GNF and its customers or participating utilities, and nothing contained in this document shall be construed as changing that contract. The use of this information by anyone for any purpose other than that for which it is intended is not authorized; and with respect to any unauthorized use, GNF-A makes no representation or warranty, and assumes no liability as to the completeness, accuracy, or usefulness of the information contained in this document.

Table of Contents

1. Introduction

This document describes one hundred-ninety (190) Light Water Reactor (LWR) critical benchmark experiment evaluations performed with the Los Alamos Monte Carlo transport code MCNP4A (Reference1). All experiments were low-enriched (5% 235U or less) UO2 pin lattice in water experiments. Fifty-two of the experiments contained UO2 rods with Gadolinium burnable absorber (Gd2O3) while seventy-seven contained other (non-fuel) structural materials such as stainless steel, Boral, borated steel and aluminum commonly found in spent fuel storage racks. All 190 experiments had material and geometric properties similar to BWR fuel lattices (not including fission product inventories) and are used to benchmark and validate the application of MCNP for both spent fuel criticality safety analyses and BWR lattice physics predictions. In addition, several include comparisons of MCNP to measured axial and radial fission density distributions.

The GE proprietary version (Reference 2) of MCNP4A (called MCNP01A) run on the GNFA cluster network was used with ENDF/B-V point-wise continuous energy cross-sections. A majority (127) of the experiments used in this report are taken from the International Criticality Safety Benchmark Evaluation Project (ICSBEP) handbook (Reference 3). Not all the experiments described in the handbook are used in this report since some lacked direct applicability to BWR spent fuel lattices. These benchmark experiments chosen represent the best available, internationally accepted, benchmark evaluations currently available for use in performing criticality safety benchmark validations for low-enriched pin-lattice in water experiments with W/F ratios between 0.8 and 4.2. [[

]] None of these experiments involve the characterization of fuel lattices with actual spent fuel isotopics (i.e., fission products, actinides) since, at the time of this report, none were available.

2. Critical Experiment Descriptions

2.1. LEU-COMP-THERM-001

This series of eight extrapolated critical experiments involving lattices composed of U(2.35%)O_2 pins in a large water tank performed (Figure 2-1) at the Pacific Northwest Laboratory (PNL) in the late 1970's. These experiments included three (3) rectangular clusters of pins arranged on a square pitch of 2.032 cm and are described in detail in References 4-6.

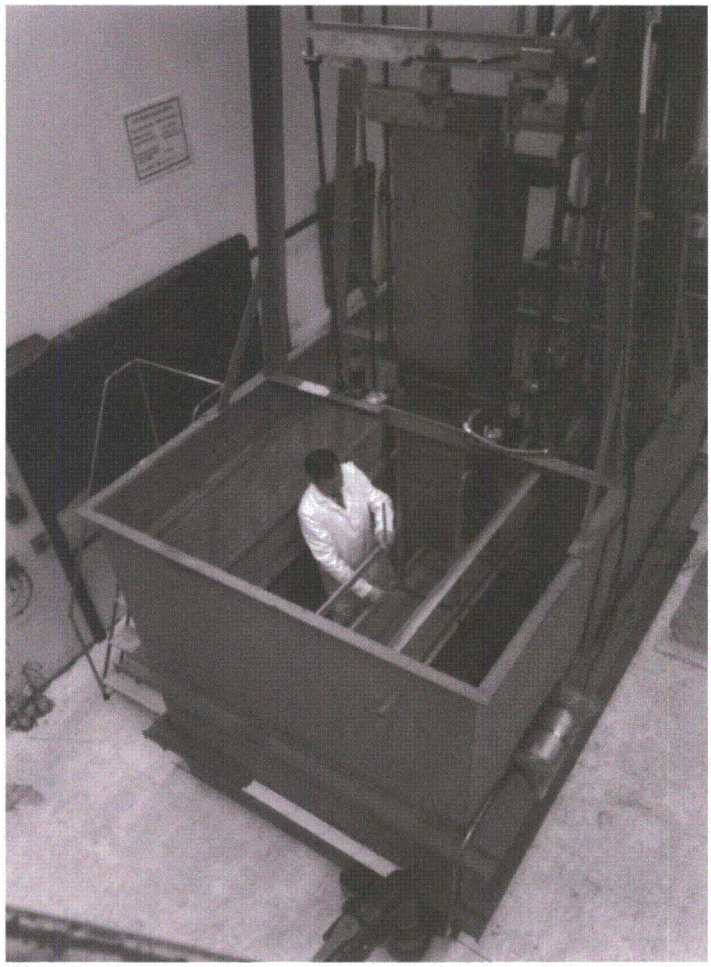

Figure 2-1.

PNL Critical Mass Laboratory Experimental Water Tank

The fuel pins used in the experiments were 1.1176 cm in diameter and 91.44 cm in active length clad in 6061 Aluminum with an OD of 1.27 cm and a wall thickness of 0.0762 cm. Figure 2-2 provides a schematic picture of the fuel rod.

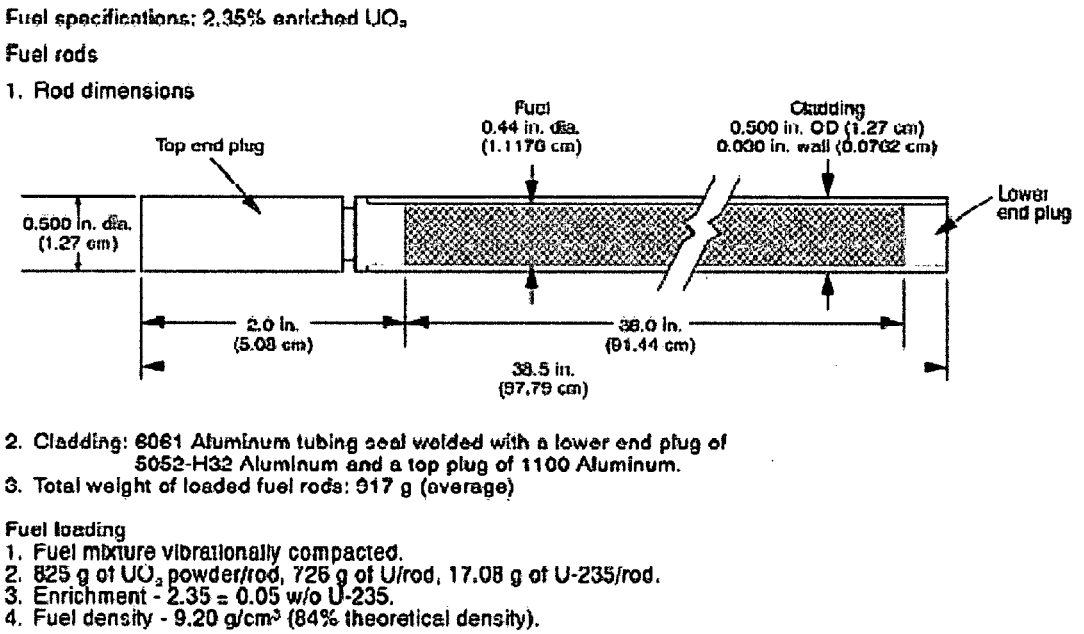

Figure 2-2.

U(2.35%)O_2 Fuel Rod

Different arrangements of pin clusters (19x16, 20x14, 20x15, 20x16, 20x17, 20x18, 22x16 and 24x15) were constructed. Then the separation distance between the clusters was reduced until a critical configuration was extrapolated. Since all fuel pins were of similar composition and size and all lattices were arranged on a 2.032cm square pitch, the effective water-to-fuel (W/F) ratio for these experiments was determined to be ~3. This makes them suitable for benchmarking BWR reactor lattice configurations.

Figure 2-3 provides a schematic description of all eight benchmark experiments showing the relative pin-lattice arrangements and water separation distances for each experiment.

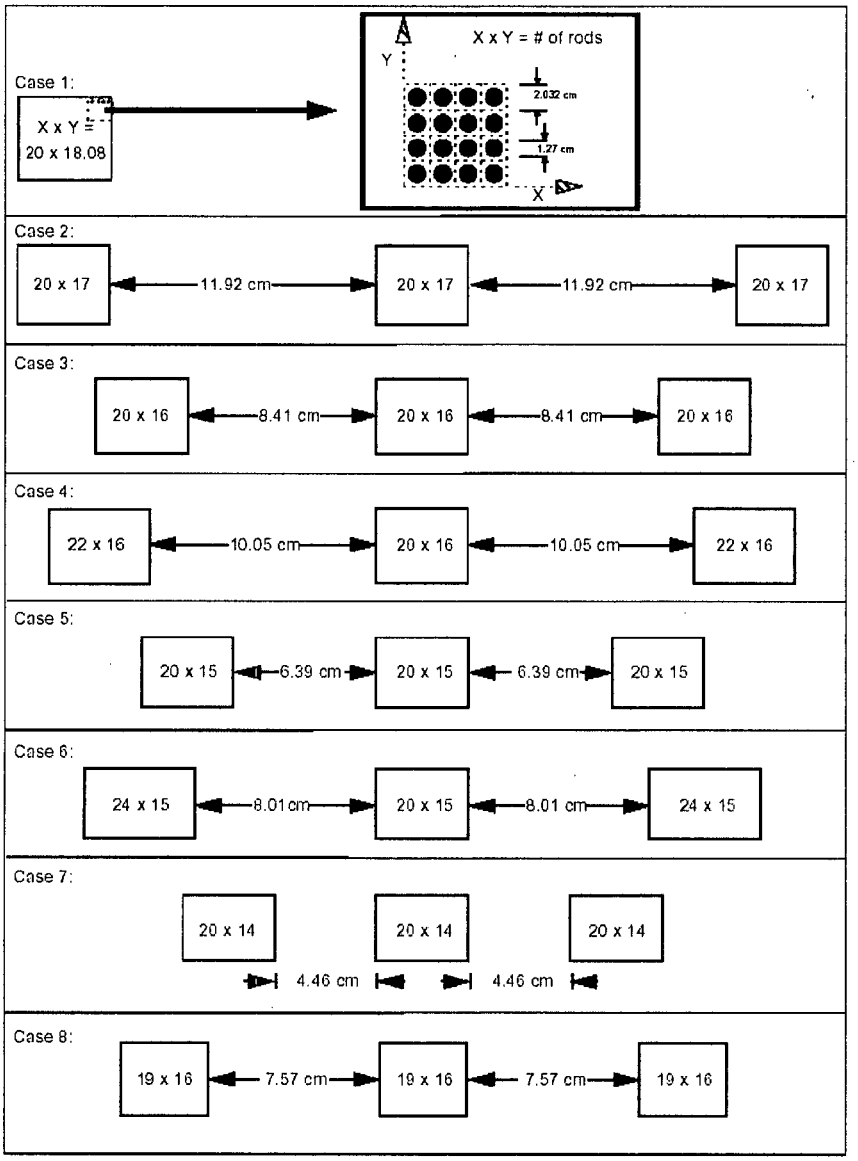

Figure 2-3.

LEU-COMP-THERM-001 Experiments

Table 2-1 provides the material atom densities used for each case. This information was taken directly from Table 9 of Reference 4 with no modification.

Table 2-1. Fuel Rod Atom Densities for LEU-COMP-THERM-001

Material	Isotope	Wt.%	Atom Density (barn-cm)$^{-1}$
U(2.35)O_2 fuel	U-234	0.0137	2.8563×10^{-6}
	U-235	2.35	4.8785×10^{-4}
	U-236	0.0171	3.5348×10^{-6}
	U-238	97.62	2.0009×10^{-2}
	O	-	4.1202×10^{-2}
1100 Aluminum (top end plug; 2.70 g/cm3)	Al	99.0	5.9660×10^{-2}
	Cu	0.12	3.0705×10^{-5}
	Mn	0.025	7.3991×10^{-6}
	Zn	0.05	1.2433×10^{-5}
	Si	0.4025	2.3302×10^{-4}
	Fe	0.4025	1.1719×10^{-4}
5052 Aluminum (lower end plug; 2.69 g/cm3)	Al	96.65	5.8028×10^{-2}
	Cr	0.25	7.7888×10^{-5}
	Cu	0.05	1.2746×10^{-5}
	Mg	2.5	1.6663×10^{-3}
	Mn	0.05	1.4743×10^{-5}
	Zn	0.05	1.2387×10^{-5}
	Si	0.225	1.2978×10^{-4}
	Fe	0.225	6.5265×10^{-5}
6061 Aluminum (clad; 2.69 g/cm3)	Al	97.325	5.8433×10^{-2}
	Cr	0.2	6.2310×10^{-5}
	Cu	0.25	6.3731×10^{-5}
	Mg	1.0	6.6651×10^{-4}
	Mn	0.075	2.2115×10^{-5}
	Ti	0.075	2.5375×10^{-5}
	Zn	0.125	3.0967×10^{-5}
	Si	0.6	3.4607×10^{-4}
	Fe	0.35	1.0152×10^{-4}

2.2. LEU-COMP-THERM-002

This series of five extrapolated critical experiments involving lattices composed of U(4.31%)O_2 pins in a large water tank performed at the Pacific Northwest Laboratory (PNL) in the late 1970's (Refs. 4-6). These experiments involved both individual and multiple (3) rectangular clusters of pins arranged on a square pitch of 2.54 cm and are similar to those performed and documented in LEU-COMP-THERM-001.

The fuel pins used in the experiments were 1.265 cm in diameter and 91.44 cm in active length clad in 6061 Aluminum with an OD of 1.415 cm and a wall thickness of 0.066 cm. Figure 2-4 provides a schematic picture of the fuel rod.

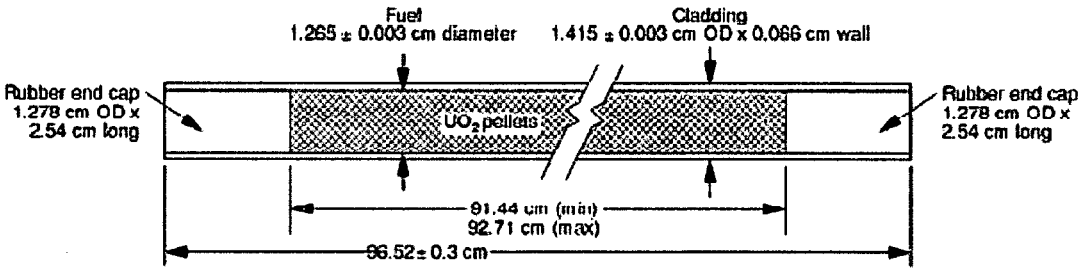

Figure 2-4.

U(4.31%)O_2 Fuel Rod

Different arrangements of pin clusters were constructed for both individual and multiple cluster configurations. Then the separation distance between the clusters was reduced until a critical configuration was extrapolated. Since all fuel pins were of similar composition and size and all lattices were arranged on a 2.54 cm square pitch, the effective water-to-fuel (W/F) ratio for these experiments was determined to be ~1.9. This makes them suitable for benchmarking BWR reactor lattice configurations.

Figure 2-5 provides a schematic description of all five benchmark experiments showing the relative pin-lattice arrangements and water separation distances for each experiment.

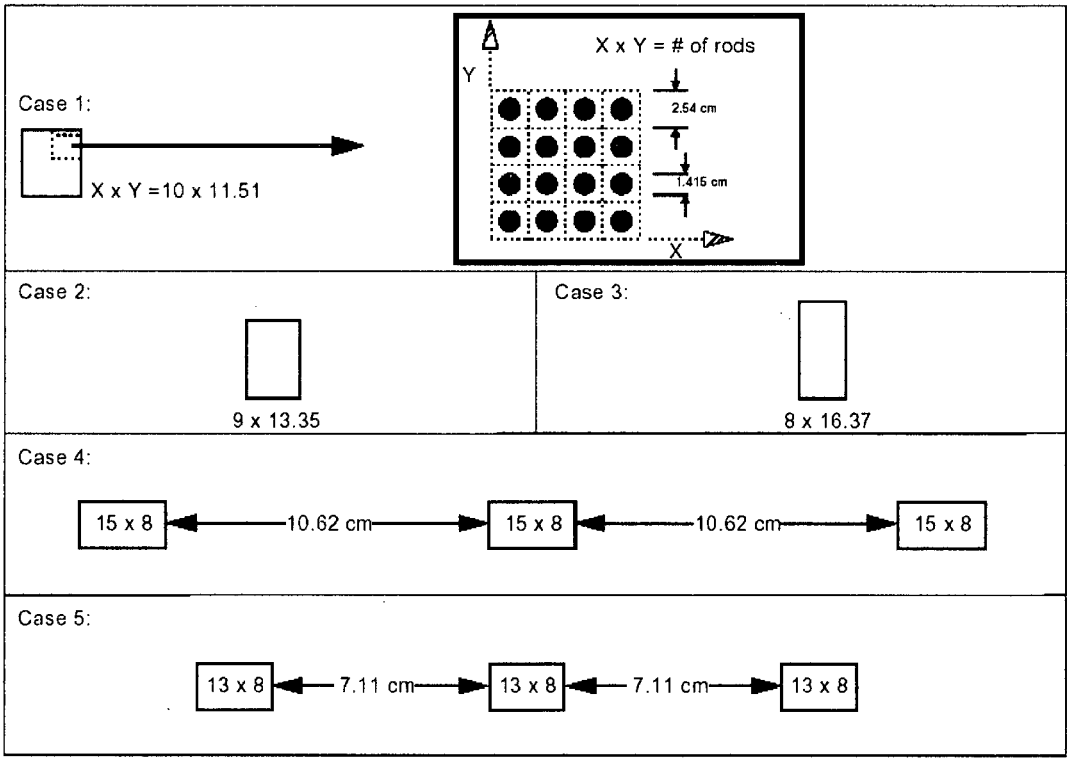

Figure 2-5.

LEU-COMP-THERM-002 Experiments

Because the critical configuration was determined by extrapolation, the critical number of rods was not an integral number (as seen in cases 2 and 3).

Tables 2-2 and 2-3 provide the material atom densities used for each case. This data was taken directly from Tables 8 and 9 of Reference 5 with no modification.

Table 2-2. Fuel Rod Atom Densities for LEU-COMP-THERM-002		
Material	Isotope	Atom Density $(barn\text{-}cm)^{-1}$
$U(4.306)O_2$ Fuel	U-234	5.1835×10^{-6}
	U-235	1.0102×10^{-3}
	U-236	5.1395×10^{-6}
	U-238	2.2157×10^{-2}
	O	4.6753×10^{-2}
6061 Aluminum Clad ($2.69\ g/cm_3$)	Al	5.8433×10^{-2}
	Cr	6.2310×10^{-5}
	Cu	6.3731×10^{-5}
	Mg	6.6651×10^{-4}
	Mn	2.2115×10^{-5}
	Ti	2.5375×10^{-5}
	Zn	3.0967×10^{-5}
	Si	3.4607×10^{-4}
	Fe	1.0152×10^{-4}
Rubber End Plug ($1.498\ g/cm_3$)	C	4.3562×10^{-2}
	H	5.8178×10^{-2}
	Ca	2.5660×10^{-3}
	S	4.7820×10^{-4}
	Si	9.6360×10^{-5}
	O	1.2461×10^{-2}

Table 2-3. Moderator-Reflector Atom Densities for LEU-COMP-THERM-002		
Material	Isotope	Atom Density $(barn\text{-}cm)^{-1}$
Water[1]	H	6.6706×10^{-2}
	O	3.3353×10^{-2}
Acrylic	H	5.6642×10^{-2}
	C	3.5648×10^{-2}
	O	1.4273×10^{-2}

[1] This is 0.997766 g/cm^3 , interpolated from densities at 20°C and 25°C 3 (CRC Handbook of Chemistry and Physics, 68th edition, p F-10.)

2.3. LEU-COMP-THERM-006

This series of eighteen critical experiments involving lattices composed of U(2.6%)O_2 pins in a large water tank performed at the Tank Critical Assembly (TCA) in Japan the late 1970's. These experiments included individual clusters of pins arranged on square pitches of 1.849, 1.956, 2.150 and 2.293 cm and are described in detail in Reference 7. Seven different basic pin cluster arrangements were used (Figure 2-6) and unique critical water level heights reported for each.

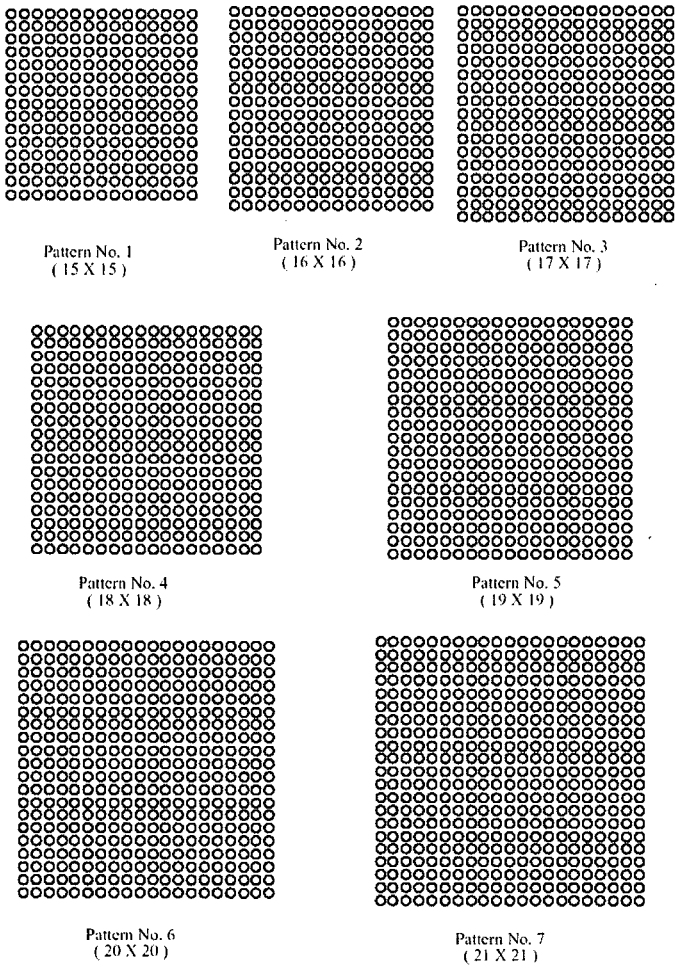

Figure 2-6.

Square Pin Cluster Arrays for LEU-COMP-THERM-006

The fuel pins used in the experiments were 1.25 cm in diameter and 144.15 cm in active length clad in Aluminum with an OD of 1.417 cm and a wall thickness of 0.076 cm. Figure 2-7 provides a schematic picture of the fuel rod.

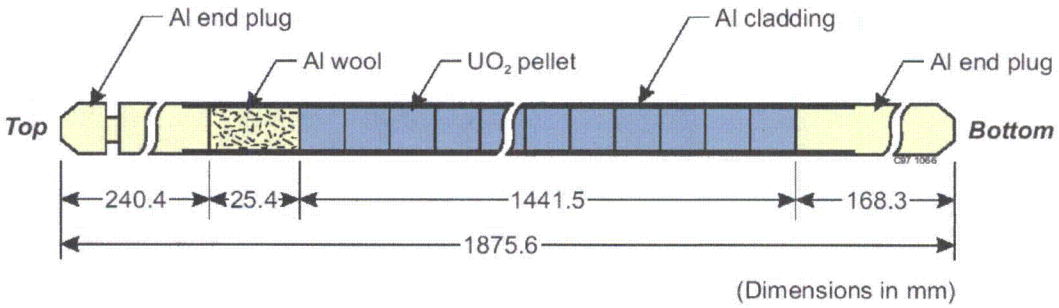

Figure 2-7.

U(2.60%)O_2 Fuel Rod

Square arrangements of pin clusters ranging from 15x15 to 21x21 were constructed at each of the four pin-lattice spacings of 1.849, 1.956, 2.150 and 2.293 cm. Then the water level height in the tank was increased until a critical configuration was achieved. Since all fuel pins were of similar composition and size and all lattices were arranged on square pitches, the effective water-to-fuel (W/F) ratio for these experiments ranged from 1.5 to 3.0. This makes them suitable for benchmarking BWR reactor lattice configurations.

Table 2-4 provides the material atom densities used for all cases. This data was taken directly from Table 14 of Reference 7 with no modification.

Table 2-4. Atom Densities for LEU-COMP-THERM-006			
Region	Material	Wt.%	Atom Density ($x10^{24}$ atoms/cm^3)
Fuel	^{234}U[2]	0.021	$4.8872x10^{-6}$
	^{235}U	2.596	$6.0830x10^{-4}$
	^{238}U	97.383	$2.2531x10^{-2}$
	O	-	$4.7214x10^{-2}$
Cladding[3]	Aluminum	-	$5.5137x10^{-2}$
Water	H	-	$6.6735x10^{-2}$
	O	-	$3.3368x10^{-2}$

[2] The fraction 0.008 x ^{235}Uwt.% was assumed.

[3] homogenized with air gap

2.4. LEU-COMP-THERM-009

This series of twenty-seven extrapolated critical experiments involving lattices composed of U(4.31%)O_2 pins in a large water tank performed at the Pacific Northwest Laboratory (PNL) in the late 1970's (Refs. 4-6). These experiments involved three rectangular clusters of pins arranged on a square pitch of 2.54 cm with steel, borated steel, Boral, copper, cadmium, aluminum and zirconium plates of varying thickness positioned in between the clusters. Of the twenty-seven experiments reported, only thirteen are judged to be acceptable as benchmarks for this validation since the experiments with copper and cadmium plates are not representative of BWR spent fuel storage configurations.

The fuel pins used in the experiments are similar to those used in LEU-COMP-THERM-002 and were 1.265 cm in diameter and 91.44 cm in active length clad in 6061 Aluminum with an OD of 1.415 cm and a wall thickness of 0.066 cm. Figure 2-8 provides a schematic picture of the fuel rod.

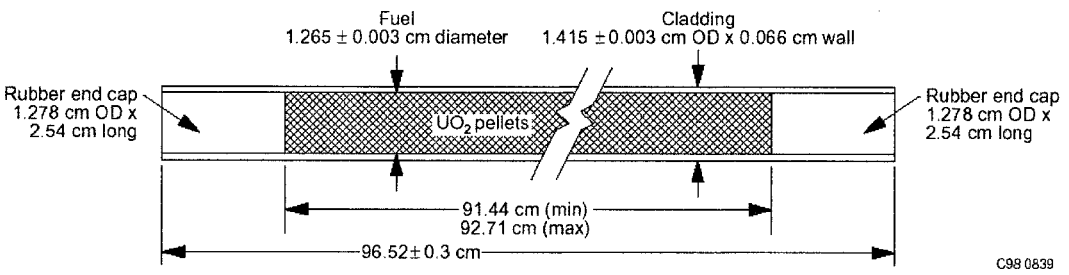

Figure 2-8.

U(4.31%)O_2 Fuel Rod

Different arrangements of pin clusters were constructed using the steel, borated steel, Boral, aluminum and zirconium plates. Then, the separation distance between the clusters was reduced until a critical configuration was extrapolated. Since all fuel pins were of similar composition and size and all lattices were arranged on a 1.892 cm square pitch, the effective water-to-fuel (W/F) ratio for these experiments was determined to be ~1.9. This makes them suitable for benchmarking BWR reactor lattice configurations inside a typical spent fuel storage rack geometry.

Figure 2-9 provides a schematic description of one of the benchmark experiments showing the relative pin-lattice arrangements, absorber plate locations and water separation distances.

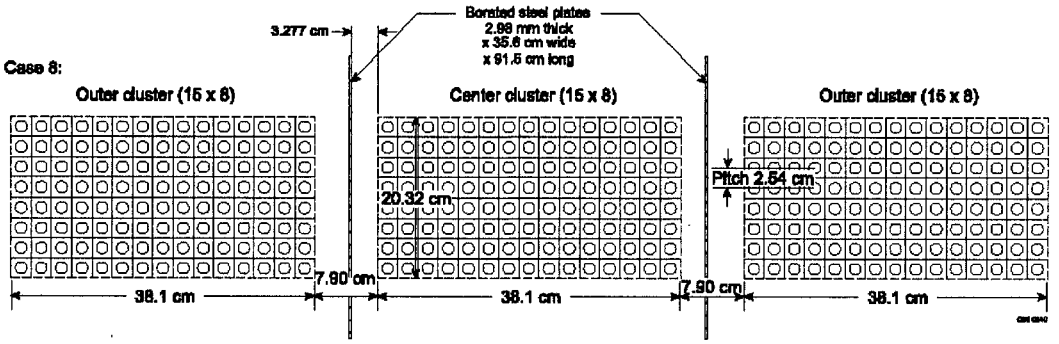

Figure 2-9.

Pin Cluster Arrays with Borated Steel Plates for LEU-COMP-THERM-009

Tables 2-5, 2-6, 2-7, 2-8, 2-9 and 2-10 provide the material atom densities used for all cases. This data was taken directly from Tables 27, 28, 29, 30, 31 and 32 of Reference 6 with no modification.

Table 2-5. Fuel-Rod Atom Densities for LEU-COMP-THERM-009		
Material	Isotope	Atom Density $(barn\text{-}cm)^{-1}$
$U(4.306)O_2$ Fuel	^{234}U	5.1835×10^{-6}
	^{235}U	1.0102×10^{-3}
	^{236}U	5.1395×10^{-6}
	^{238}U	2.2157×10^{-2}
	O	4.6753×10^{-2}
	Al	5.8433×10^{-2}
6061-Aluminum Clad ($2.69\ g/cm^3$)	Cr	6.2310×10^{-5}
	Cu	6.3731×10^{-5}
	Mg	6.6651×10^{-4}
	Mn	2.2115×10^{-5}
	Ti	2.5375×10^{-5}
	Zn	3.0967×10^{-5}
	Si	3.4607×10^{-4}
	Fe	1.0152×10^{-4}
	C	4.3562×10^{-2}
Rubber End Plug ($1.498\ g/cm^3$)	H	5.8178×10^{-2}
	Ca	2.5660×10^{-3}
	S	4.7820×10^{-4}
	Si	9.6360×10^{-5}
	O	1.2461×10^{-2}

Table 2-6. Steel Absorber-Plate Atom Densities for LEU-COMP-THERM-009			
Material	Isotope	Wt.%	Atom Density $(barn\text{-}cm)^{-1}$
304L Steel without B (7.93 g/cm^3)	Cr	18.56	1.7046×10^{-2}
	Cu	0.27	2.0291×10^{-4}
	Fe	68.24	5.8353×10^{-2}
	Mn	1.58	1.3734×10^{-3}
	Mo	0.26	1.2942×10^{-4}
	Ni	11.09	9.0238×10^{-3}
304L Steel with 1.1 wt.% B (7.9 g/cm^3)	^{10}B	1.05 wt.% boron, 19.9 at.% ^{10}B	9.1950×10^{-4}
	^{11}B	1.05 wt.% boron, 80.1 at.% ^{11}B	3.7011×10^{-3}
	Cr	19.03	1.7412×10^{-2}
	Cu	0.28	2.0963×10^{-4}
	Fe	68.04	5.7961×10^{-2}
	Mn	1.58	1.3682×10^{-3}
	Mo	0.49	2.4298×10^{-4}
	Ni	9.53	7.7251×10^{-3}
304L Steel with 1.6 wt.% B (7.77 g/cm^3)	^{10}B	1.62 wt.% boron, 19.9 at.% ^{10}B	1.3953×10^{-3}
	^{11}B	1.62 wt.% boron, 80.1 at.% ^{11}B	5.6163×10^{-3}
	Cr	19.6	1.7638×10^{-2}
	Cu	0.26	1.9145×10^{-4}
	Fe	66.4	5.5634×10^{-2}
	Mn	1.69	1.4394×10^{-3}
	Mo	0.31	1.5119×10^{-4}
	Ni	10.12	8.0684×10^{-3}

Table 2-7. Boral Absorber-Plate Atom Densities for LEU-COMP-THERM-009			
Material	Isotope	Wt.%	Atom Density
B_4C-Al[4] (2.49 g/cm3)	Al	62.39	3.4673×10^{-2}
	^{10}B	28.7 wt.% boron, 19.9 at. % ^{10}B	7.9217×10^{-3}
	^{11}B	28.7 wt.% boron, 80.1 at. % ^{11}B	3.1886×10^{-2}
	C	7.97	9.9501×10^{-3}
	Cr	0.05	1.4419×10^{-5}
	Cu	0.09	2.1237×10^{-5}
	Fe	0.33	8.8606×10^{-5}
	Mg	0.05	3.0848×10^{-5}
	Mn	0.05	1.3647×10^{-5}
	Na	0.02	1.3045×10^{-5}
	Ni	0.02	5.1099×10^{-6}
	Si	0.2	1.0678×10^{-4}
	S	0.03	1.4027×10^{-5}
	Zn	0.1	2.2932×10^{-5}
1100 Aluminum[5] (2.70 g/cm^3)	Al	99.0	5.9660×10^{-2}
	Cu	0.12	3.0705×10^{-5}
	Mn	0.025	7.3991×10^{-6}
	Zn	0.05	1.2433×10^{-5}
	Si	0.4025	2.3302×10^{-4}
	Fe	0.4025	1.1719×10^{-4}

[4] middle 0.509-cm thickness of plate

[5] 0.102-cm-thick clad on both sides of B4C-Al

Table 2-8. Copper Absorber-Plate Atom Densities for LEU-COMP-THERM-009			
Material	Isotope	Wt.%	Atom Density
Copper without Cd (8.913 g/cm^3)	C	0.34	1.5194×10^{-3}
	Cu	99.6	8.4128×10^{-2}
	Fe	0.004	3.8444×10^{-6}
	Mg	0.002	4.4168×10^{-6}
	Na	0.002	4.6695×10^{-6}
	O	0.03	1.0064×10^{-4}
	Si	0.02	3.8223×10^{-5}
	S	0.002	3.3474×10^{-6}
Copper with Cd (8.910 g/cm^3)	^{10}B	0.005 wt.% boron, 19.9 at.% ^{10}B	4.9384×10^{-6}
	^{11}B	0.005 wt.% boron, 80.1 at.% ^{11}B	1.9878×10^{-5}
	C	0.002	8.9346×10^{-6}
	Cd	0.989	4.7208×10^{-4}
	Cu	98.685	8.3328×10^{-2}
	Fe	0.02	1.9216×10^{-5}
	Mn	0.009	8.7901×10^{-6}
	Ni	0.01	9.1424×10^{-6}
	O	0.019	6.3720×10^{-5}
	Si	0.004	7.6419×10^{-6}
	Sn	0.25	1.1300×10^{-4}
	Zn	0.007	5.7440×10^{-6}

Table 2-9. Cadmium, Aluminum, and Zircaloy-4 Absorber-Plate Atom Densities for LEU-COMP-THERM-009			
Material	Isotope	Wt.%	Atom Density $(barn\text{-}cm)^{-1}$
Cadmium	Cd	99.7	4.6201×10^{-2}
($8.65\ g/cm^3$)	Zn	0.3	2.3899×10^{-4}
Aluminum	Al	97.15	5.8371×10^{-2}
($2.692\ g/cm^3$)	Cr	0.21	6.5475×10^{-5}
	Cu	0.12	3.0614×10^{-5}
	Fe	0.82	2.3803×10^{-4}
	Mn	0.21	6.1968×10^{-5}
	Si	0.82	4.7332×10^{-4}
	S	0.06	3.0330×10^{-5}
	Ti	0.61	2.0654×10^{-4}
Zircaloy-4	Zr	98.16	4.0953×10^{-2}
($6.32\ g/cm^3$)	Fe	0.21	1.4311×10^{-4}
	Sn	1.5	4.8092×10^{-4}
	Cr	0.13	9.5156×10^{-5}

Table 2-10. Moderator-Reflector Atom Densities for LEU-COMP-THERM-009		
Material	Isotope	Atom Density $(barn\text{-}cm)^{-1}$
Water	H	6.6675×10^{-2}
	O	3.3338×10^{-2}
Acrylic	H	5.6642×10^{-2}
	C	3.5648×10^{-2}
	O	1.4273×10^{-2}

2.5. LEU-COMP-THERM-016

This series of thirty-two extrapolated critical experiments involving lattices composed of U(2.35%)O_2 pins in a large water tank performed at the Pacific Northwest Laboratory (PNL) in the late 1970's (Refs. 4-6). These experiments involved three rectangular clusters of pins arranged on a square pitch of 2.032 cm with steel, Boral, copper, cadmium, aluminum and zircalloy-4 plates of varying thickness positioned in between the clusters. Of the thirty-two experiments reported, only twenty are judged to be acceptable as benchmarks for this validation since the experiments with copper and cadmium plates are not representative of BWR spent fuel storage configurations.

The fuel pins used in the experiments are similar to those used in LEU-COMP-THERM-001 and were 1.1176 cm in diameter and 91.44 cm in active length clad in 6061 Aluminum with an OD of 1.27 cm and a wall thickness of 0.0762 cm. Figure 2-10 provides a schematic picture of the fuel rod.

Fuel specifications: 2.35% enriched UO_2

Fuel rods
1. Rod dimensions

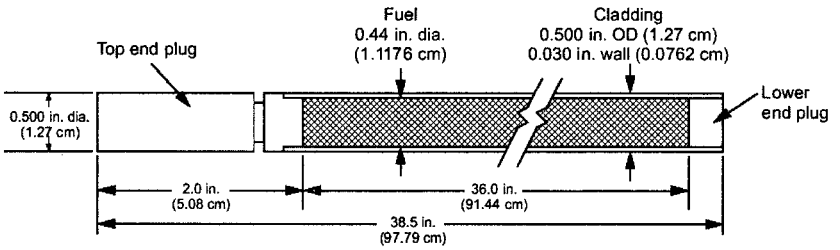

2. Cladding: 6061 Aluminum tubing seal welded with a lower end plug of 5052-H32 Aluminum and a top plug of 1100 Aluminum.
3. Total weight of loaded fuel rods: 917 g (average)

Fuel loading
1. Fuel mixture vibrationally compacted.
2. 825 g of UO_2 powdered/rod, 726 g of U/rod, 17.08 g of U-235/rod.
3. Enrichment = 2.35 ± 0.05 w/o U-235.
4. Fuel density = 9.20 g/cm (84% theoretical density).

C98 0171

Figure 2-10.

U(2.35%)O_2 Fuel Rod

Different arrangements of pin clusters were constructed using the steel, borated steel, Boral, aluminum and zircalloy-4 plates. Then, the separation distance between the clusters was reduced until a critical configuration was extrapolated. Since all fuel pins were of similar composition and size and all lattices were arranged on a 2.032 cm square pitch, the effective water-to-fuel (W/F) ratio for these experiments was determined to be ~3.2. This makes them suitable for benchmarking BWR reactor lattice configurations inside a typical spent fuel storage rack geometry.

Figure 2-11 provides a schematic description of one of the benchmark experiments showing the relative pin-lattice arrangements, absorber plate locations and water separation distances.

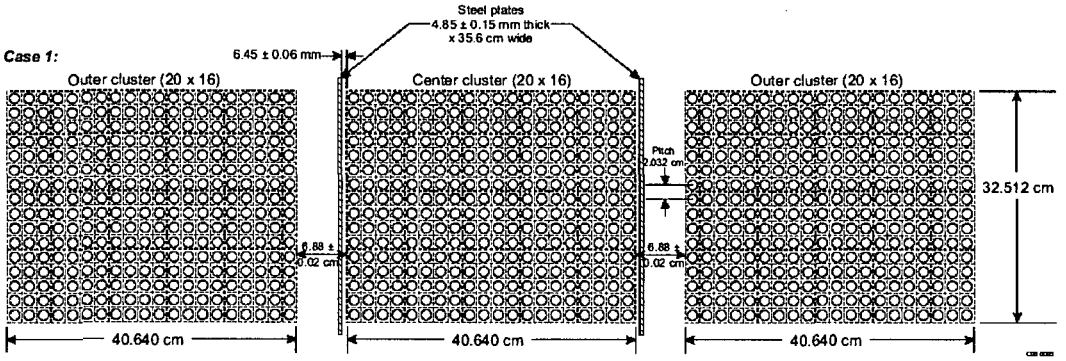

Figure 2-11.

Pin Cluster Arrays with Steel Plates for LEU-COMP-THERM-016

Tables 2-11, 2-12, 2-13, 2-14 and 2-15 provide the material atom densities used for all cases. This data was taken directly from Tables 34, 35, 36, 37 and 38 of Reference 6 with no modification.

Table 2-11. Fuel Rod Atom Densities for LEU-COMP-THERM-016			
Material	Isotope	Wt.%	Atom Density (barn-cm)-1
UO_2 Fuel	^{234}U	---	2.8563×10^{-6}
	^{235}U	---	4.8785×10^{-4}
	^{236}U	---	3.5348×10^{-6}
	^{238}U	---	2.0009×10^{-2}
	O	---	4.1202×10^{-2}
1100 Aluminum (top end plug; 2.70 g/cm^3)	Al	99.0	5.9660×10^{-2}
	Cu	0.12	3.0705×10^{-5}
	Mn	0.025	7.3991×10^{-6}
	Zn	0.05	1.2433×10^{-5}
	Si	0.4025	2.3302×10^{-4}
	Fe	0.4025	1.1719×10^{-4}
5052 Aluminum (lower end plug; 2.69 g/cm^3)	Al	96.65	5.8028×10^{-2}
	Cr	0.25	7.7888×10^{-5}
	Cu	0.05	1.2746×10^{-5}
	Mg	2.5	1.6663×10^{-3}
	Mn	0.05	1.4743×10^{-3}
	Zn	0.05	1.2387×10^{-5}
	Si	0.225	1.2978×10^{-4}
	Fe	0.225	6.5265×10^{-5}
6061 Aluminum (clad; 2.69 g/cm^3)	Al	97.325	5.8433×10^{-2}
	Cr	0.2	6.2310×10^{-5}
	Cu	0.25	6.3731×10^{-5}
	Mg	1.0	6.6651×10^{-4}
	Mn	0.075	2.2115×10^{-5}
	Ti	0.075	2.5375×10^{-5}
	Zn	0.125	3.0967×10^{-5}
	Si	0.6	3.4607×10^{-4}
	Fe	0.35	1.0152×10^{-4}

Table 2-12. Steel Absorber-Plate Atom Densities for LEU-COMP-THERM-016			
Material	Isotope	Wt.%	Atom Density (barn-cm)-1
304L Steel without B ($7.93\ g/cm^3$)	Cr	18.56	1.7046×10^{-2}
	Cu	0.27	2.0291×10^{-4}
	Fe	68.24	5.8353×10^{-2}
	Mn	1.58	1.3734×10^{-3}
	Mo	0.26	1.2942×10^{-4}
	Ni	11.09	9.0238×10^{-3}
304L Steel with 1.1 wt.% B ($7.9\ g/cm^3$)	10B	1.05 x 0.18431	9.1950×10^{-4}
	11B	1.05 x 0.81569	3.7011×10^{-3}
	Cr	19.03	1.7412×10^{-2}
	Cu	0.28	2.0963×10^{-2}
	Fe	68.04	5.7961×10^{-2}
	Mn	1.58	1.3682×10^{-2}
	Mo	0.49	2.4298×10^{-4}
	Ni	9.53	7.7251×10^{-3}
304L Steel with 1.6 wt.% B ($7.77\ g/cm^3$)	10B	1.62 x 0.18431	1.3953×10^{-3}
	11B	1.62 x 0.81569	5.6163×10^{-3}
	Cr	19.6	1.7638×10^{-2}
	Cu	0.26	1.9145×10^{-4}
	Fe	66.4	5.5634×10^{-2}
	Mn	1.69	1.4394×10^{-3}
	Mo	0.31	1.5119×10^{-4}
	Ni	10.12	8.0684×10^{-3}

Table 2-13. Boral/Copper Plate Atom Densities for LEU-COMP-THERM-016			
Material	Isotope	Wt.%	Atom Density
Boral (2.49 g/ cm^3)	Al	62.39	3.4673×10^{-2}
	^{10}B	28.7 x 0.18431	7.9217×10^{-3}
	^{11}B	28.7 x 0.81569	3.1886×10^{-2}
	C	7.97	9.9501×10^{-3}
	Cr	0.05	1.4419×10^{-5}
	Cu	0.09	2.1237×10^{-5}
	Fe	0.33	8.8606×10^{-5}
	Mg	0.05	3.0848×10^{-5}
	Mn	0.05	1.3647×10^{-5}
	Na	0.02	1.3045×10^{-5}
	Ni	0.02	5.1099×10^{-6}
	Si	0.2	1.0678×10^{-4}
	S	0.03	1.4027×10^{-5}
	Zn	0.1	2.2932×10^{-5}
Copper with Cd (8.910 g/ cm^3)	^{10}B	0.005 x 0.18431	4.9384×10^{-6}
	^{11}B	0.005 x 0.81569	1.9878×10^{-6}
	C	0.002	8.9346×10^{-6}
	Cd	0.989	4.7208×10^{-4}
	Cu	98.685	8.3328×10^{-2}
	Fe	0.02	1.9216×10^{-5}
	Mn	0.009	8.7901×10^{-6}
	Ni	0.01	9.1424×10^{-6}
	O	0.019	6.3720×10^{-5}
	Si	0.004	7.6419×10^{-6}
	Sn	0.25	1.1300×10^{-4}
	Zn	0.007	5.7440×10^{-6}
Copper without Cd (8.913 g/ cm^3)	C	0.34	1.5194×10^{-3}
	Cu	99.6	8.4128×10^{-2}
	Fe	0.004	3.8444×10^{-6}
	Mg	0.002	4.4168×10^{-6}
	Na	0.002	4.6695×10^{-6}
	O	0.03	1.0064×10^{-4}
	Si	0.02	3.8223×10^{-5}
	S	0.002	3.3474×10^{-6}

Table 2-14. Cadmium, Aluminum, and Zircaloy Absorber-Plate Atom Densities for LEU-COMP-THERM-016			
Material	Isotope	Wt.%	Atom Density (barn-cm)-1
Cadmium ($8.65\ g/cm^3$)	Cd	99.7	4.6201×10^{-2}
	Zn	0.3	2.3899×10^{-4}
Aluminum ($2.692\ g/cm^3$)	Al	97.15	5.8371×10^{-2}
	Cr	0.21	6.5475×10^{-5}
	Cu	0.12	3.0614×10^{-5}
	Fe	0.82	2.3803×10^{-4}
	Mn	0.21	6.1968×10^{-5}
	Si	0.82	4.7332×10^{-4}
	S	0.06	3.0330×10^{-5}
	Ti	0.61	2.0654×10^{-4}
Zircaloy-4 ($6.32\ g/cm^3$)	Zr	98.16	4.0953×10^{-2}
	Fe	0.21	1.4311×10^{-4}
	Sn	1.5	4.8092×10^{-4}
	Cr	0.13	9.5156×10^{-5}

Table 2-15. Moderator-Reflector Atom Densities for LEU-COMP-THERM-016		
Material	Isotope	Atom Density (barn-cm)-1
Water	H	6.6743×10^{-2}
	O	3.3371×10^{-2}
Acrylic	H	5.6642×10^{-2}
	C	3.5648×10^{-2}
	O	1.4273×10^{-2}

2.6. LEU-COMP-THERM-034

This series of twenty-six critical experiments involving lattices composed of U(4.738%)O_2 pins in a large water tank performed at the Valduc facility in France in the early 1980's (Reference 8). These experiments involved four individual 18x18 pin clusters (each with a square pitch of 1.6 cm) arranged on a table-top surface. The pin-clusters were then outfitted with square canisters of borated stainless steel, Boral and cadmium placed over them while the critical water level height was determined for a variety of cluster separation distances. Figure 2-12 shows a picture of the four clusters (without canisters) sitting on the table-top surface.

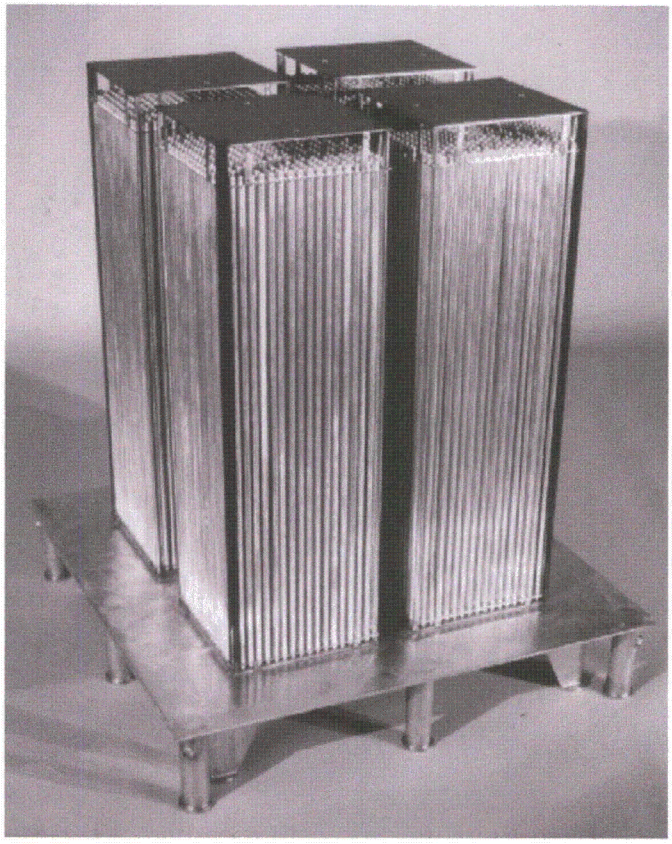

Figure 2-12.

Valduc Experimental Configuration

Of the twenty-six experiments reported, only fifteen are judged to be acceptable as benchmarks for this validation since the experiments with cadmium canisters are not representative of BWR spent fuel storage configurations.

The fuel pins used in the experiments were 0.79 cm in diameter and 90 cm in active length clad in Aluminum with an OD of 0.94 cm and a wall thickness of 0.06 cm. Figure 2-13 provides a schematic picture of the fuel rod.

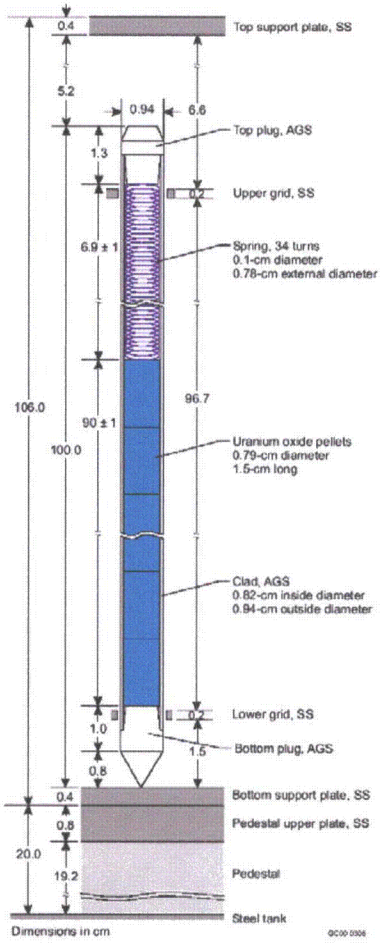

Figure 2-13.

U(4.738%)O_2 Fuel Rod in Support Plate Structure

The array of four 18x18 pin-clusters was changed by re-positioning the lattices on the table-top at different separation distances with and without the borated stainless steel and boral canister covers. Then, the tank water level height was increased until a critical configuration was achieved. Since all fuel pins were of similar composition and size and all lattices were arranged on a 1.6 cm square pitch, the effective water-to-fuel (W/F) ratio for these experiments was determined to be ~4.2. This makes them suitable for benchmarking BWR reactor lattice configurations inside a typical spent fuel storage rack geometry.

Figure 2-14 provides a schematic description of one of the benchmark experiments showing the relative pin-lattice arrangements, absorber plate locations and water separation distances.

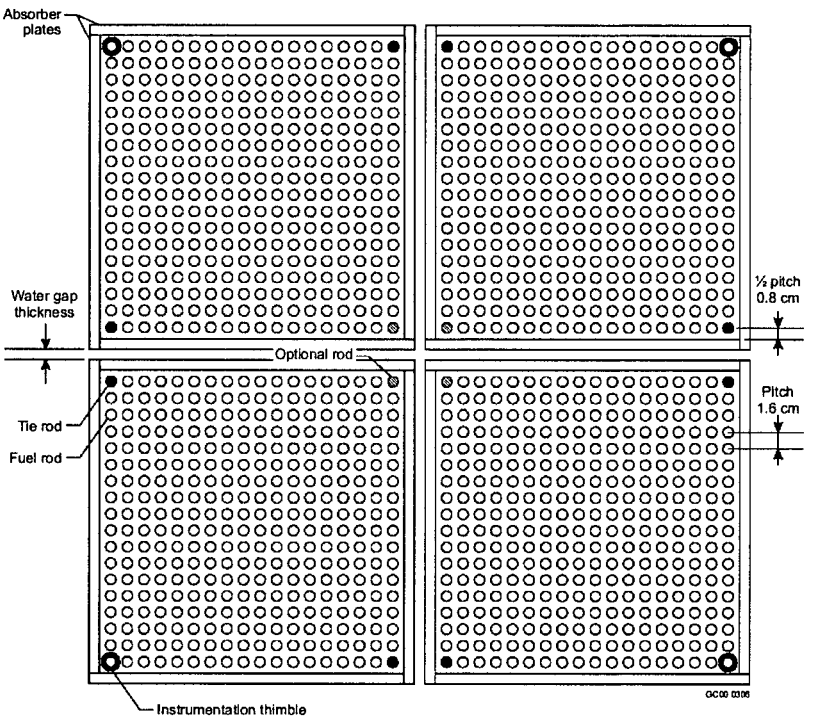

Figure 2-14.

Pin Cluster Arrays with Canister for LEU-COMP-THERM-034

Tables 2-16 and 2-17 provide the material atom densities used for all cases. This data was taken directly from Tables 13 and 14 of Reference 8 with no modification.

Table 2-16. Atom Densities for Basic Materials for LEU-COMP-THERM-034 (atoms/barn-cm)

UO_2	^{234}U	7.1318×10^{-6}
	^{235}U	1.1104×10^{-3}
	^{236}U	3.1838×10^{-5}
	^{238}U	2.2006×10^{-2}
	O	4.6391×10^{-2}
	^{10}B	5.7531×10^{-8}
	^{11}B	2.3157×10^{-7}
Water (22 °C)	H	6.6707×10^{-2}
	O	3.3354×10^{-2}
Aluminum Alloy AGS (clad, plugs)	Al	5.9569×10^{-2}
	Mg	3.1442×10^{-4}
	Si	2.4894×10^{-4}
	Fe	6.4052×10^{-5}
	Zn	7.4597×10^{-6}
Stainless Steel Z2 CN18/10[1] (support plates, grid plates, tie rods, instrumentation thimbles, cover for cadmium plates)	Fe	5.8694×10^{-2}
	Cr	1.6469×10^{-2}
	Ni	8.1061×10^{-3}
	Mn	1.7319×10^{-3}
	Si	1.6939×10^{-3}
	P	6.1438×10^{-5}
	S	4.4504×10^{-5}
	C	1.1883×10^{-4}

Table 2-17. Atom Densities for Absorber Materials for LEU-COMP-THERM-034 (atoms/barn-cm).		
Borated Steel	Fe	5.7220×10^{-2}
	Cr	1.7203×10^{-2}
	Ni	1.0707×10^{-2}
	Mn	5.9877×10^{-4}
	Si	1.0507×10^{-3}
	P	4.6855×10^{-5}
	S	9.0506×10^{-6}
	C	1.4499×10^{-4}
	^{10}B	9.7950×10^{-4}
	^{11}B	3.9426×10^{-3}
Aluminum [6]	Al	5.9169×10^{-2}
B4C + Al [7]	C	8.0894×10^{-3}
	Al	4.1873×10^{-2}
	^{10}B	6.4448×10^{-3}
	^{11}B	2.5941×10^{-2}
Cadmium	Cd	4.6340×10^{-2}

[6] 0.11-cm-thick Boral external plates.

[7] 0.43-cm-thick internal absorbing sheet of Boral.

2.7. LEU-COMP-THERM-039

This series of seventeen critical experiments involving lattices composed of U(4.738%)O_2 pins in a large water tank performed at the Valduc facility in France in the early 1980's (Reference 9). These experiments involved a single 22x22 (or 21x21) pin cluster array (each with a square pitch of 1.26 cm) arranged on a table-top surface. These experiments are categorized as "incomplete array" geometries since selected fuel pins were removed from the lattice in a particular sequence or pattern and the critical water level height re-established for each case. Figure 2-15 shows a picture of the rod cluster sitting on the table-top surface.

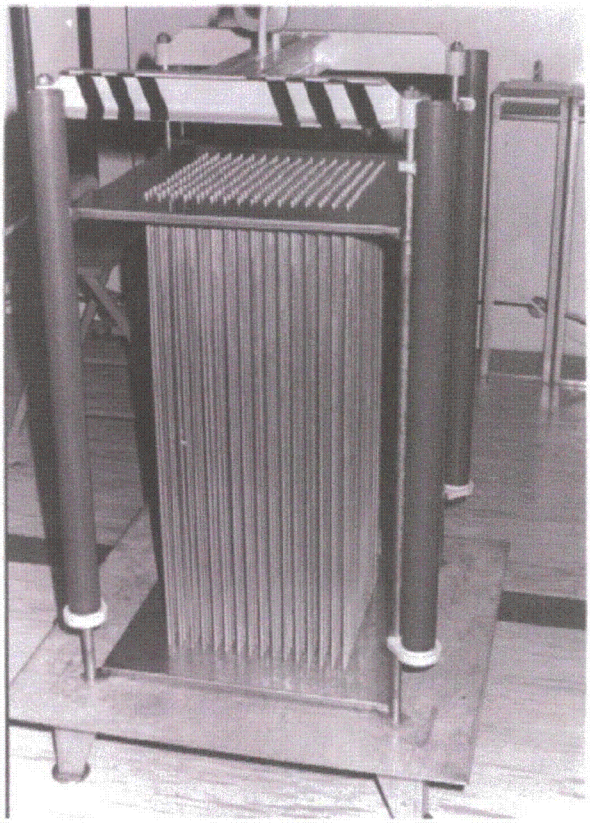

Figure 2-15.

Valduc Experimental Configuration

Of the seventeen experiments reported, all are judged to be acceptable as benchmarks for this validation report.

The fuel pins used in the experiments are similar to those described in LEU-COMP-THERM-034 and were 0.79 cm in diameter and 90 cm in active length clad in Aluminum with an OD of 0.94 cm and a wall thickness of 0.06 cm. Figure 2-16 provides a schematic picture of the fuel rod.

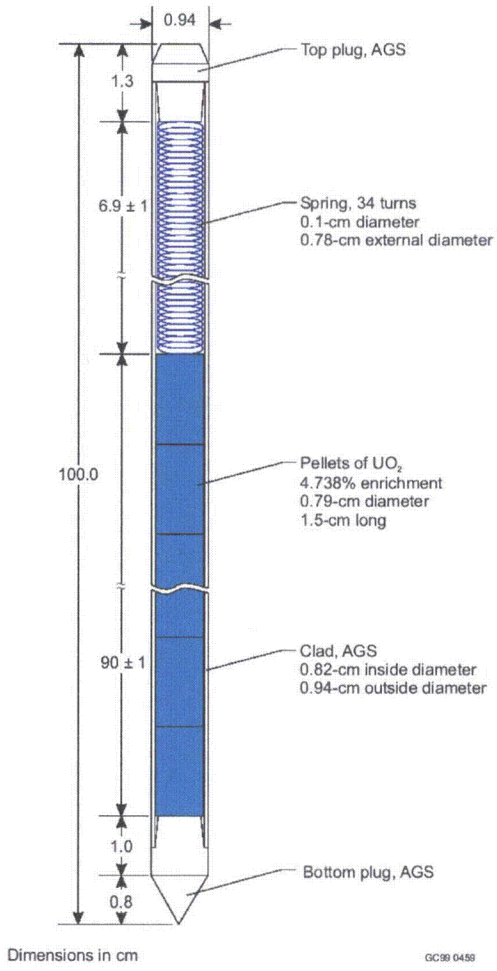

Figure 2-16.

U(4.738%)O_2 Fuel Rod

Fifteen of the seventeen experiments were performed with an incomplete 22x22 pin array while the remaining two were performed with a 21x21 array. After each experiment, a different group of fuel rods was removed/replaced from the array in a particular pattern. Then, the tank was flooded and the water level height was increased until a critical configuration was achieved. Although all fuel pins were of similar composition and size and all lattices were arranged on a 1.26 cm square pitch, the effective water-to-fuel (W/F) ratio inside the array varied depending on the number of rods removed from the array during each experiment. The W/F ratio for these seventeen experiments is calculated to vary from 2.4 to 3.4. This makes them suitable for benchmarking BWR reactor lattice configurations.

Figure 2-17 provides a schematic description of several of the incomplete array configurations created during the experiments. This set of experiments are particularly relevant to BWR reactor lattices since the incomplete array configurations look quite similar to the vanished lattice arrays frequently analyzed in spent fuel criticality safety analyses.

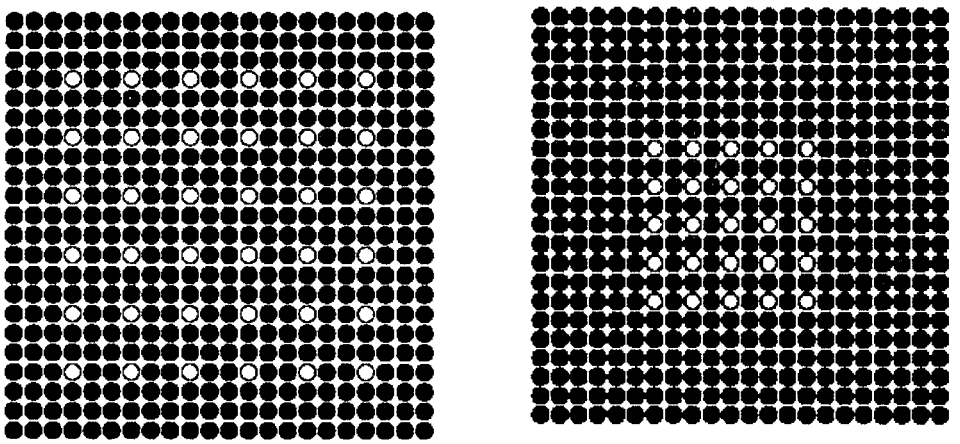

Figure 2-17.

Schematic of Two Incomplete Array Configurations

Table 2-18 provides the material atom densities used for all cases. This data was taken directly from Table 9 of Reference 9 with no modification.

Table 2-18. Atom Densities for Basic Materials for LEU-COMP-THERM-039 (atoms/barn-cm)		
UO_2	^{235}U	1.1104×10^{-3}
	^{238}U	2.2006×10^{-2}
	^{234}U	7.1318×10^{-6}
	^{236}U	3.1838×10^{-5}
	O	4.6391×10^{-2}
	^{10}B	5.7531×10^{-8}
	^{11}B	2.3157×10^{-7}
AGS (clad, plugs)	Al	5.9569×10^{-2}
	Mg	3.1442×10^{-4}
	Si	2.4894×10^{-4}
	Zn	7.4597×10^{-6}
	Fe	6.4052×10^{-5}
Air	N	4.1805×10^{-5}
	O	1.2633×10^{-5}
Water Density = 0.9980[8]	O	3.3353×10^{-2}
	H	6.6706×10^{-2}
Stainless steel (grid, pedestal plate)	C	1.1883×10^{-4}
	Cr	1.6469×10^{-2}
	Fe	5.8694×10^{-2}
	Mn	1.7319×10^{-3}
	Ni	8.1061×10^{-3}
	Si	1.6939×10^{-3}
	S	4.4504×10^{-5}
	^{31}P	6.1438×10^{-5}

[8] at 22 °C.

2.8. LEU-COMP-THERM-062

This series of fifteen critical experiments involving lattices composed of $U(2.6\%)O_2$ pins in a large water tank performed at the Tank Critical Assembly (TCA) in Japan the early 1990's (Reference 7). These experiments involved a single, 18x18 rod cluster array of fuel pins (1.9558 cm pitch) with and without a single borated stainless plate of varying thickness and boron content adjacent to the rod cluster. Figure 2-18 shows a schematic picture of the array with a borated stainless steel plate.

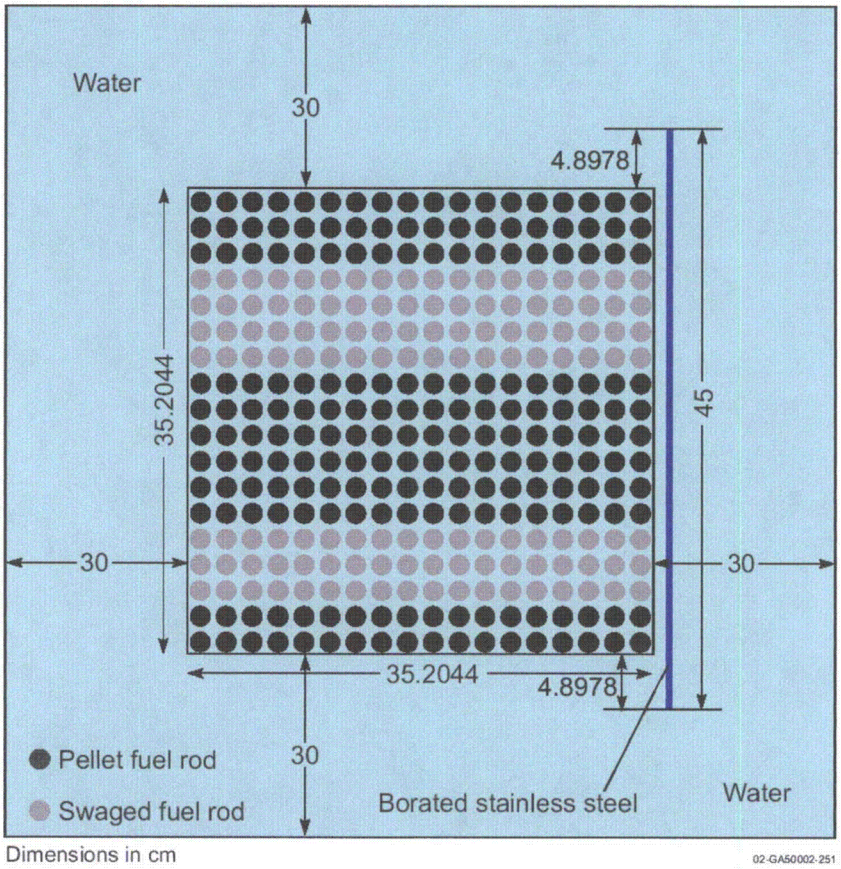

Figure 2-18.

Schematic of Array with Borated Stainless Steel Plate

Of the fifteen experiments reported, all are judged to be acceptable as benchmarks for this validation report.

The fuel pins used in the experiments were manufactured by GE in the early 1960's and were 1.2502 cm in diameter and 144.15 cm in active length clad in Aluminum with an OD of 1.4172 cm and a wall thickness of 0.0762 cm. Figure 2-19 provides a schematic picture of the pellet (top) and swaged (bottom) fuel rods used in the experiments.

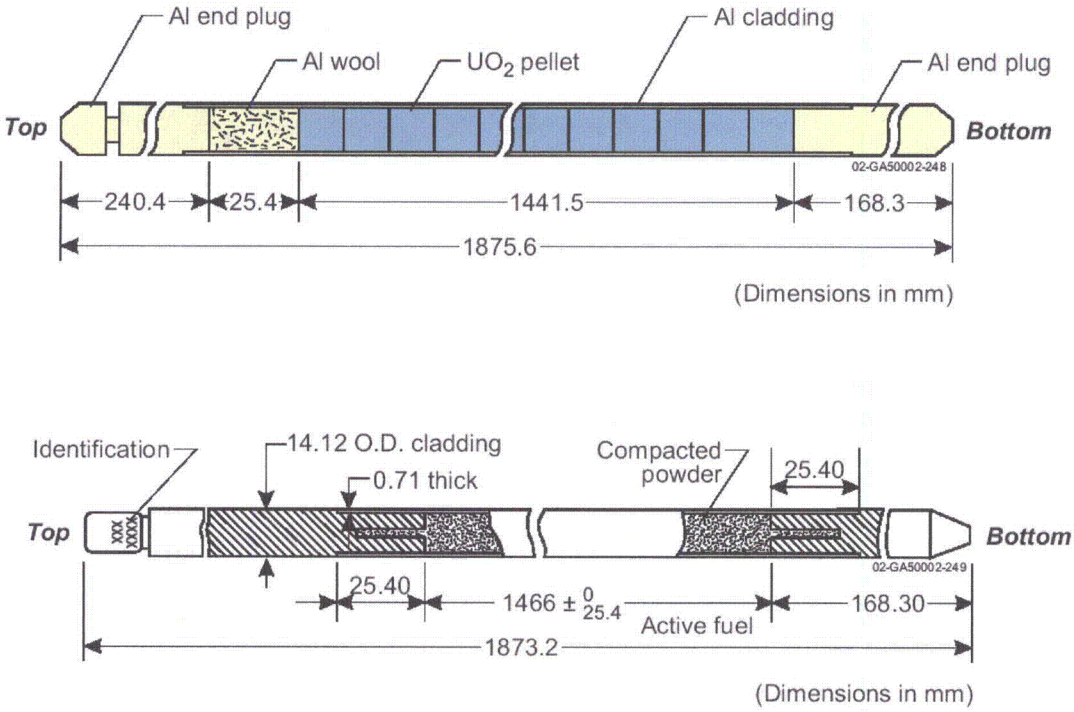

Figure 2-19.

Pellet and Swaged Fuel Rods

Six of the experiments were performed with 0.67 wt.% boron stainless steel plates with two different plate thicknesses of 0.3114 and 0.6228 cm. Four were performed with 0 wt.% boron stainless steel plates with plate thicknesses of 0.2910 and 0.5820 cm. Four were performed with 0.98 wt.% stainless steel plates with plate thicknesses of 0.3097 and 0.6194 cm. One experiment was performed with no plate at all. The critical water level height was established for each unique combination of stainless steel plate wt.% boron, plate thickness and spacing between the plate and the rod array cluster. Since all fuel pins were of similar composition and size and all lattices were arranged on a 1.9558 cm square pitch, the effective water-to-fuel (W/F) ratio inside the array was ~2.1. In addition, the stainless steel and borated stainless steel plate thicknesses are representative of typical spent fuel storage rack cell dimensions and compositions. This makes them suitable for benchmarking BWR reactor lattice configurations inside a spent fuel storage rack geometry.

Tables 2-19, 2-20, 2-21, 2-22, 2-23 and 2-24 provide the material atom densities used for all cases. This data was taken directly from Tables 19, 20, 21, 22, 23 and 24 of Reference 7 with no modification.

Table 2-19. Fuel Atom Densities for LEU-COMP-THERM-062			
Material	Isotope	Isotopic composition (wt.%)	Atom density (barn-cm)$^{-1}$
UO_2 Pellet	^{234}U	0.0208	4.8825×10^{-6}
	^{235}U	2.60	6.0771×10^{-4}
	^{238}U	97.3792	2.2474×10^{-2}
	O	-	4.7002×10^{-2}
UO_2 Powder	^{234}U	0.0206	4.6478×10^{-6}
	^{235}U	2.58	5.7850×10^{-4}
	^{238}U	97.3994	2.1564×10^{-2}
	O	-	4.4367×10^{-2}

Table 2-20. Atom Densities of 6061 Aluminum Alloy for LEU-COMP-THERM-062			
Material	Element	Wt.%	Atom density (barn-cm)$^{-1}$
Cladding, top and bottom end plugs, upper and lower grid plates, support plate (density 2.69 g/cm^3)	Al	97.325	5.8433×10^{-2}
	Cr	0.2	6.2310×10^{-5}
	Cu	0.25	6.3731×10^{-5}
	Mg	1.0	6.6651×10^{-4}
	Mn	0.075	2.2115×10^{-5}
	Ti	0.075	2.5375×10^{-5}
	Zn	0.125	3.0967×10^{-5}
	Si	0.6	3.4607×10^{-4}
	Fe	0.35	1.0152×10^{-4}

Table 2-21. Atom Densities of Stainless Steel for LEU-COMP-THERM-062		
Material	Element	Atom density (barn-cm)$^{-1}$
	C	1.1928×10^{-4}
	Si	1.7003×10^{-3}
Lower support	Mn	1.7385×10^{-3}
plate	P	6.9381×10^{-5}
S.S.304L[(a)]	S	4.4673×10^{-5}
(SUS304L)	Ni	8.9509×10^{-3}
	Cr	1.7450×10^{-2}
	Fe	5.7202×10^{-2}

Table 2-22. Atom Densities of Stainless Steel Plate for LEU-COMP-THERM-062			
Material	Element	Wt.%	Atom density (barn-cm)$^{-1}$
Stainless steel, boron content 0 wt.% density 7.932 g/cm^3	C	0.06	2.3862×10^{-4}
	Si	0.45	7.6534×10^{-4}
	Mn	0.83	7.2165×10^{-4}
	P	0.026	4.0096×10^{-5}
	S	0.008	1.1916×10^{-5}
	Cr	18.23	1.6747×10^{-2}
	Ni	8.70	7.0807×10^{-3}
	Fe	71.696	6.1322×10^{-2}

Table 2-23. Atom Density of 0.67-Wt.%-Borated Stainless Steel Plate for LEU-COMP-THERM-062				
Material	Element	Wt.%	Atom density (barn-cm)-1	
Stainless steel Boron content 0.67 wt.% Density 7.799 g/cm^3	C	0.01525	5.9632×10^{-5}	
	Si	0.7275	1.2166×10^{-3}	
	Mn	1.785	1.5260×10^{-3}	
	P	0.0255	3.8666×10^{-5}	
	S	0.001	1.4645×10^{-6}	
	Cr	19.715	1.7808×10^{-2}	
	Ni	9.955	7.9664×10^{-3}	
	Mo	0.575	2.8148×10^{-4}	
	B	0.67	^{10}B	5.7923×10^{-4}
			^{11}B	2.3315×10^{-3}
	Fe	66.53075	5.5951×10^{-2}	

Table 2-24. Atom Density of 0.98-Wt.%-Borated Stainless Steel Plate for LEU-COMP-THERM-062				
Material	Element	Wt.%	Atom density (barn-cm)-1	
Stainless steel Boron content 0.9825 wt.% Density 7.815 g/cm^3	C	0.01	3.9183×10^{-5}	
	Si	0.435	7.2893×10^{-4}	
	Mn	1.6675	1.4285×10^{-3}	
	P	0.01125	1.7094×10^{-5}	
	S	0.00375	5.5031×10^{-6}	
	Cr	19.3475	1.7512×10^{-2}	
	Ni	10.1625	8.1492×10^{-3}	
	Mo	0.6	2.9433×10^{-4}	
	B	0.9825	^{10}B	8.5113×10^{-4}
			^{11}B	3.4259×10^{-3}
	Fe	66.78	5.6276×10^{-2}	

2.9. LEU-COMP-THERM-065

This series of seventeen critical experiments involving lattices composed of U(2.6%)O_2 pins in a large water tank performed at the Tank Critical Assembly (TCA) in Japan the early 1990's (Reference 10). These experiments involved two, 18x18 rectangular rod array clusters (1.9558 cm pitch) with and without double borated stainless plates of varying thickness and boron content in between the rod clusters. Figure 2-20 shows a schematic picture of the arrays with a borated stainless steel plates in between. These experiments are very similar to those documented in LEU-COMP-THERM-062 as both used the same pellet and swaged fuel pin types.

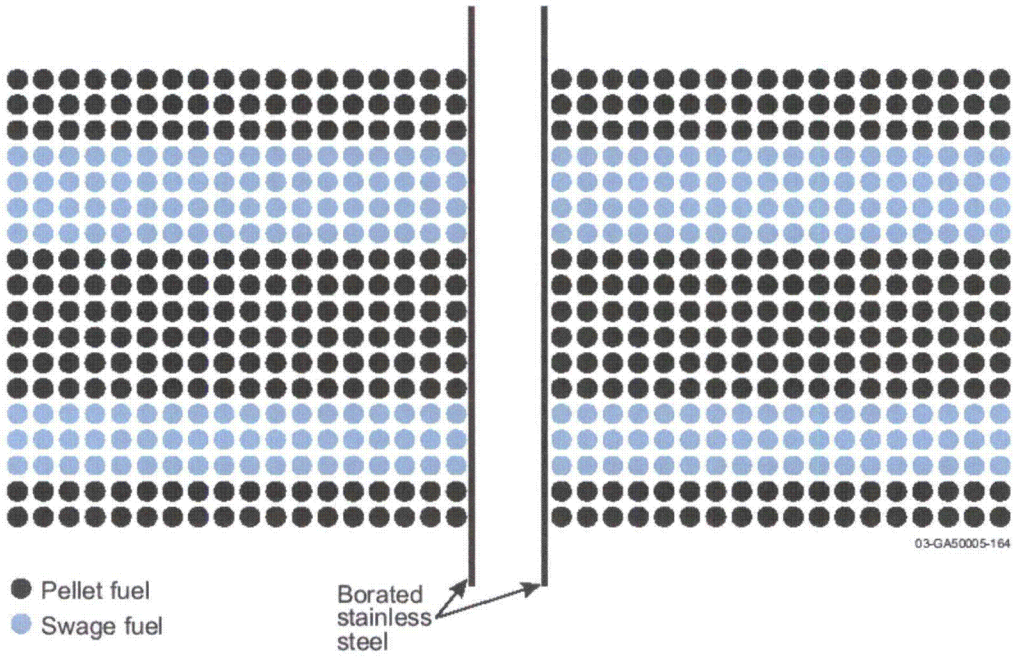

Figure 2-20.

Schematic of Arrays with Borated Stainless Steel Plates

Of the seventeen experiments reported, all are judged to be acceptable as benchmarks for this validation report. The pellet and swaged fuel pins are identical to those specified in LEU-COMP-THERM-062 in Figure 2-19 of this document.

Five of the experiments were performed with 0.0 wt.% boron stainless steel plates with two different plate thicknesses of 0.2910 and 0.5820 cm. Five were performed with 0.67 wt.% boron stainless steel plates with plate thicknesses of 0.3114 and 0.6228 cm. Five were performed with 0.98 wt.% stainless steel plates with plate thicknesses of 0.3097 and 0.6194 cm. Two experiments were performed with no plates at all. The critical water level height was established for each unique combination of stainless steel plate wt.% boron, plate thickness, spacing between the plate and the rod array cluster and spacing between the rod array cluster and the symmetry plane. Since all fuel pins were of similar composition and size and all lattices were arranged on a 1.9558 cm square pitch, the effective water-to-fuel (W/F) ratio inside the array was ~2.1. In addition, the stainless steel and borated stainless steel plate thicknesses are representative of typical spent fuel storage rack cell dimensions and compositions. This makes them suitable for benchmarking BWR reactor lattice configurations inside a spent fuel storage rack geometry.

Tables 2-25, 2-26, 2-27, 2-28, 2-29 and 2-30 provide the material atom densities used for all cases. This data was taken directly from Tables 19, 20, 21, 22, 23 and 24 of Reference 10 with no modification.

Table 2-25. Fuel Rod Atom Densities for LEU-COMP-THERM-065			
Material	Isotope	Isotopic Composition (wt.%)	Atom Density (barn-cm)$^{-1}$
Pellet-type UO_2	^{234}U	0.0208	4.8902×10^{-6}
	^{235}U	2.60	6.0867×10^{-4}
	^{238}U	97.3792	2.2509×10^{-2}
	O	-	4.7076×10^{-2}
Swage-type UO_2	^{234}U	0.02064	4.6611×10^{-6}
	^{235}U	2.58	5.8015×10^{-4}
	^{238}U	97.39936	2.1625×10^{-2}
	O	-	4.4493×10^{-2}

Table 2-26. Atom Density of 6061 Aluminum Alloy			
Material	Element	Wt.%	Atom Density (barn-cm)$^{-1}$
Cladding	Al	97.325	5.8433×10^{-2}
	Cr	0.2	6.2310×10^{-5}
Top and bottom end plug	Cu	0.25	6.3731×10^{-5}
	Mg	1.0	6.6651×10^{-4}
Upper and lower grid plate	Mn	0.075	2.2115×10^{-5}
Support plate	Ti	0.075	2.5375×10^{-5}
	Zn	0.125	3.0967×10^{-5}
Density 2.69 g/cm^3	Si	0.6	3.4607×10^{-4}
	Fe	0.35	1.0152×10^{-4}

Table 2-27. Atom Densities of Stainless Steel		
Material	Element	Atom Density (barn-cm)$^{-1}$
Support plate S.S.304L (SUS304L)	C	1.1928×10^{-4}
	Si	1.7003×10^{-3}
	Mn	1.7385×10^{-3}
	P	6.9381×10^{-5}
	S	4.4673×10^{-5}
	Ni	8.9509×10^{-3}
	Cr	1.7450×10^{-2}
	Fe	5.7202×10^{-2}

Table 2-28. Atom Density of Stainless Steel Absorber Plate			
Material	Element	Wt.%	Atom Density (barn-cm)$^{-1}$
Stainless Steel Boron Content 0 wt.% Density 7.932 g/cm^3	C	0.06	2.3862×10^{-4}
	Si	0.45	7.6534×10^{-4}
	Mn	0.83	7.2165×10^{-4}
	P	0.026	4.0096×10^{-5}
	S	0.008	1.1916×10^{-5}
	Cr	18.23	1.6747×10^{-2}
	Ni	8.70	7.0807×10^{-3}
	Fe	71.696	6.1322×10^{-2}

Table 2-29. Atom Density of Borated Stainless Steel Plate (0.67 wt.% boron content)				
Material	Element	Wt.%		Atom density (barn-cm)$^{-1}$
Stainless steel Boron content 0.67 wt.% Density 7.799 g/cm^3	C	0.01525		5.9632×10^{-5}
	Si	0.7275		1.2166×10^{-3}
	Mn	1.785		1.5260×10^{-3}
	P	0.0255		3.8666×10^{-5}
	S	0.001		1.4645×10^{-6}
	Cr	19.715		1.7808×10^{-2}
	Ni	9.955		7.9664×10^{-3}
	Mo	0.575		2.8148×10^{-4}
	B	0.67	^{10}B	5.7923×10^{-4}
			^{11}B	2.3315×10^{-4}
	Fe	66.53075		5.5951×10^{-2}

Table 2-30. Atom Density of Borated Stainless Steel Plate (0.9825 wt.% boron content).				
Material	Element	Wt.%		Atom Density (barn-cm)$^{-1}$
Stainless Steel Boron Content 0.9825 wt.% Density 7.815 g/cm^3	C	0.01		3.9183×10^{-5}
	Si	0.435		7.2893×10^{-4}
	Mn	1.6675		1.4285×10^{-3}
	P	0.01125		1.7094×10^{-5}
	S	0.00375		5.5031×10^{-6}
	Cr	19.3475		1.7512×10^{-2}
	Ni	10.1625		8.1492×10^{-3}
	Mo	0.6		2.9433×10^{-4}
	B	0.9825	^{10}B	8.5113×10^{-4}
			^{11}B	3.4259×10^{-3}
	Fe	66.78		5.6276×10^{-2}

2.10. Jersey Central Criticals with and without Poison Curtains

[[

]]

[[

]]

Figure 2-21.
1/8-Core Symmetry Model of Jersey Central Experiments

[[

]]

Figure 2-22.

Jersey Central Bundles and Spacing

[[

]]

[[		
		]]

2.11. Small Core Criticals with Burnable Absorbers (KRITZ-75)

[[

]]

[[

]]

Figure 2-23.

KRITZ-75 Half-Core Symmetry Model

[[

]]

Figure 2-24.

KRITZ-75 Bundle Configuration

[[

]]

[[

			]]

2.12. NCA Step II & III Criticals

[[

]]

[[

]]

Figure 2-25.

Schematic of the NCA Tank Facility

[[

]]

Figure 2-26.

Schematic of the Step II & III Test Zone Lattices

[[

]]

[[

]]

[[			
			]]

* Smeared atom densities are used for consistency with TGBLA.

[[

			]]

[[			
			]]

2.13. NCA GNF1 Criticals

[[

]]

[[

]]

Figure 2-27.

[[ ]]

[[

]]

[[

		]]

3. MCNP and the Monte Carlo Method

The version of the MCNP Monte Carlo code used in this benchmark validation study is MCNP01A (the GE level 02 version of MCNP4A). MCNP is a generalized Monte Carlo program for solving the linear neutron transport equation as a fixed source or an eigenvalue problem in three space dimensions. It implements the Monte Carlo process for neutron, photon or electron transport, or coupled transport involving all these particles, and can compute the eigenvalue for neutron-multiplying systems. For the present application only neutron transport was considered.

MCNP uses point-wise (i.e., continuous energy) cross section data, and all reactions in a given cross section evaluation (e.g., ENDF/B-V) are considered. For the present work, thermal neutron scattering with hydrogen was described using an S(α,β) light water thermal scattering kernel. The cross section tables include all details of the ENDF representations for neutron data. The code requires that all the cross-sections be given on a single union energy grid suitable for linear interpolation; however, the cross section energy grid varies from isotope to isotope. The libraries include very little data thinning and utilize maximum resonance integral reconstruction error tolerances of 0.001 %.

MCNP implements a robust geometry representation that can correctly model complex components in three dimensions. An arbitrary three-dimensional configuration is treated as geometric cells bounded by first and second-degree surfaces. The cells are described in a Cartesian coordinate system and are defined by the intersections, unions and complements of the regions bounded by the surfaces. Surfaces are defined by supplying coefficients to the analytic surface equations or, for certain types of surfaces, known points on the surfaces. Rather than combining several pre-defined geometrical bodies in a combinatorial geometry scheme, MCNP has the flexibility of defining geometrical shapes from all the first and second-degree surfaces of analytical geometry and then combining them with Boolean operators. The code performs extensive checking for geometry errors and provides a plotting feature for examining the geometry and material assignments.

4. Monte Carlo Simulation Results

Prior to discussing the results of the benchmark simulation models, it is appropriate to identify the methods and techniques used by the International Criticality Safety Benchmark Evaluation Project to quantify and evaluate both experimental and calculational uncertainties which can affect a code and cross-section data sets ability to reproduce an observed critical condition.

In each of the ICSBEP benchmark experiments, Section 2.0 (Evaluation of Experimental Data) and Section 3.0 (Benchmark Model Specifications) are included. These sections describe in detail all of the evaluated experimental uncertainties and their potential impact on the predicted critical eigenvalue via sensitivity studies evaluating each of the most important independent variables of the experiment. The experimental variables evaluated with sensitivity studies are provided in Table 4-1.

The benchmark models used in this study represent the best-estimate representations of each experiment given all the uncertainties analyzed in Table 4-1. For all ICSBEP benchmark cases, a total of 10,000 neutron histories per batch were executed for a total of 500 batches with the first 50 batches not included in the eigenvalue estimation average. [[

]] In all cases, the MCNP01A output was carefully examined to ensure proper convergence of the fission source before eigenvalue averaging was performed for the final results. In addition, all three eigenvalue estimators (collision, absorption and track length) were confirmed to be normally distributed within the 95% confidence interval.

Table 4-1 - Experimental Variables Evaluated for Sensitivity Studies

Experiment	Parameter(s)	Δk
LEU-COMP-THERM-001	Fuel enrichment, diameter, length, clad thickness, pitch, uranium mass	±0.30%
	Water Reflector thickness	< 0.004%
	Water temperature	±0.005%
	Cluster separation	0.04% - 0.09%
LEU-COMP-THERM-002	Fuel length, plug compression, fuel diameter, pitch, enrichment	+0.13% -0.18%
	Water Reflector thickness	< 0.002%
	Water temperature	±0.04%
	Cluster separation	0.01% - 0.04%
LEU-COMP-THERM-006	Fuel enrichment, density, pellet diameter, clad diameter, clad thickness, pitch	±0.16%
	Grid plates, detectors, source	< 0.001%
	Critical water level height, water temperature	0.01% - 0.08%
LEU-COMP-THERM-009	Fuel length, pin diameter, pitch, enrichment	±0.18%
	Water Reflector thickness	< 0.002%
	Water temperature	±0.04%
	Cluster separation	< 0.011%
	Absorber plate separation	< 0.013%
	Vertical position of absorber plates	±0.078%
	Absorber plate composition	< 0.023%
	Absorber plate thickness	< 0.013%
LEU-COMP-THERM-016	Fuel enrichment, diameter, length, clad thickness, pitch, uranium mass	+0.31% -0.30%
	Water Reflector thickness	< 0.002%
	Water impurities	< 0.004%
	Water temperature	±0.008%
	Cluster separation	±0.001%
	Absorber plate separation	±0.002%
	Absorber plate composition	< 0.017%
	Absorber plate thickness	< 0.002%
LEU-COMP-THERM-034	Rod array	0.0066%
	Absorber plate thickness	0.00257%
	Absorber plate thickness and composition	< 0.00098%
	Configuration uncertainties	< 0.00206%
LEU-COMP-THERM-039	Boron impurity in fuel	0.00036%
	Impurities in water	0.00005%
	Fuel enrichment, pin pitch, cladding OD, fuel pin OD, temperature, UO2 density, fuel height, moderator height	0.0014%
LEU-COMP-THERM-062	Enrichment, fuel pin OD, UO2 mass, clad thickness, fuel length, pellet OD, lattice pitch, random spacing of larger holes	0.138%
	Borated SS plate thickness	< 0.004%
	Borated SS plate B-10 content	< 0.009%
	Borated SS plate B content	< 0.008%
	Borated SS plate gap width	< 0.056%
	Critical water level height	< 0.005%
	Water temperature	< 0.003%
LEU-COMP-THERM-065	Enrichment, fuel pin OD, UO2 mass, clad thickness, fuel length, pellet OD, lattice pitch, random spacing of larger holes	0.132%
	Borated SS plate thickness	< 0.004%
	Borated SS plate B-10 content	< 0.013%
	Borated SS plate B content	< 0.006%
	Borated SS plate gap width	< 0.085%
	Critical water level height	< 0.005%
	Water temperature	< 0.003%

4.1. LEU-COMP-THERM-001 Results

The benchmark models for these experiments were created based on the generic MCNP input model provided in Appendix A.2 of LEU-COMP-THERM-001. All of the material composition atom density data used in the models was taken directly from Table 9 of the LEU-COMP-THERM-001 for consistency with the internationally recognized experimental evaluation.

A total of eight experiments were modeled. For the cases involving three pin clusters, the separation distances between the clusters ranged from 4.46 cm to 11.92 cm. The system was full water reflected on all six sides by at least 12 inches of water. All calculations were performed with material and cross-section data representative of the system at 20°C. The Benchmark model k_{eff} was 0.9998±0.0031 for these experiments.

Table 4-2 presents the results of the benchmark model comparisons for MCNP using both ENDF/B-V evaluated nuclear data. For all eight cases, the active fuel pin radius of 0.5588 cm and the square lattice pitch of 2.032 cm resulted in an effective (W/F) ratio of 3.209.

Table 4-2 - Benchmark Results for LEU-COMP-THERM-001

Case	# Clusters	Cluster Dim. (# Rods)	Cluster Separation (cm)	$K_{eff} \pm 1\sigma$
1	1	20x18.08	N/A	[[
2	3	20x17	11.92	
3	3	20x16	8.41	
4	3	20x16 (center) 22x16 (outer)	10.05	
5	3	20x15	6.39	
6	3	20x15 (center) 22x15 (outer)	8.01	
7	3	20x14	4.46	
8	3	19x16	7.57	]]

4.2. LEU-COMP-THERM-002 Results

The benchmark models for these experiments were created based on the generic MCNP input model provided in Appendix A.2 of LEU-COMP-THERM-002. All of the material composition atom density data used in the models was taken directly from the Table 8 of the LEU-COMP-THERM-002 for consistency with the internationally recognized experimental evaluation.

A total of five experiments were modeled. The system was full water reflected on all six sides by at least 12 inches of water. All calculations were performed with material and cross-section data representative of the system at 20°C. The Benchmark model k_{eff} was 0.9997±0.002 for these experiments.

Table 4-3 presents the results. For all five cases, the active fuel pin radius of 0.6325 cm and the square lattice pitch of 1.892 cm resulted in an effective (W/F) ratio of 1.848.

Table 4-3 - Benchmark Results for LEU-COMP-THERM-002

Case	# Clusters	Cluster Dim. (# Rods)	Cluster Separation (cm)	$K_{eff} \pm 1\sigma$
1	1	10x11.51	N/A	[[
2	1	9x13.35	N/A	
3	1	8x16.37	N/A	
4	3	15x8	10.62	
5	3	13x8	7.11	]]

4.3. LEU-COMP-THERM-006 Results

The benchmark models for these experiments were created based on the generic MCNP input model provided in Appendix A.2 of LEU-COMP-THERM-006. All of the material composition atom density data used in the models was taken directly from the Table 14 of the LEU-COMP-THERM-006 for consistency with the internationally recognized experimental evaluation. This data was checked for consistency and is shown as Table 4-4 below.

A total of eighteen experiments were modeled. The system was full water reflected on all six sides by at least 12 inches of water. All calculations were performed with material and cross-section data representative of the system at 20°C. The Benchmark model k_{eff} was 1.000±0.002 for these experiments.

Table 4-4 presents the results. For all eighteen cases, the active fuel pin radius of 0.625 cm was constant but experiments were performed for four different square lattice pitches of 1.849 cm, 19.56 cm, 2.150 cm and 2.293 cm. The corresponding (W/F) ratios are given along with the lattice pitch (cm) and critical water height (Hc) in cm with each result.

Table 4-4 - Benchmark Results for LEU-COMP-THERM-006

Case	Pitch	Hc	$K_{eff} \pm 1\sigma$	W/F	Case	Pitch	Hc	$K_{eff} \pm 1\sigma$	W/F
1	1.849	99.45	0.99598±0.00034	1.50	10	2.150	59.96	[[	2.48
2	1.849	73.73	0.99630±0.00034	1.50	11	2.150	50.52		2.48
3	1.849	60.81	0.99543±0.00036	1.50	12	2.150	44.45		2.48
4	1.956	114.59	0.99580±0.00033	1.83	13	2.150	40.44		2.48
5	1.956	75.32	0.99652±0.00034	1.83	14	2.293	90.75		3.00
6	1.956	60.38	0.99660±0.00035	1.83	15	2.293	64.42		3.00
7	1.956	51.65	0.99668±0.00033	1.83	16	2.293	52.87		3.00
8	1.956	46.01	0.99680±0.00034	1.83	17	2.293	46.06		3.00
9	2.150	78.67	0.99764±0.00033	2.48	18	2.293	41.54	]]	3.00

4.4. LEU-COMP-THERM-009 Results

The benchmark models for these experiments were created based on the generic MCNP input model provided in Appendix A.2 of LEU-COMP-THERM-009. All of the material composition atom density data used in the models was taken directly from the Table 27 of the LEU-COMP-THERM-009 for consistency with the internationally recognized experimental evaluation.

A total of thirteen experiments were modeled. The system was full water reflected on all six sides by at least 12 inches of water. All calculations were performed with material and cross-section data representative of the system at 20°C. The Benchmark model k_{eff} was 1.000±0.0021 for these experiments.

Table 4-5 presents the results. For all thirteen cases, the active fuel pin radius of 0.6325 cm and the square lattice pitch of 1.892 cm resulted in an effective (W/F) ratio of 1.848.

Table 4-5 - Benchmark Results for LEU-COMP-THERM-009

Case	Plate Type	Plate Thks. (mm)	Distance to Center Cluster (mm)	Cluster Separation (mm)	$K_{eff} \pm 1\sigma$
1	0% B	4.85±0.15	2.45±0.33	85.8±0.2	[[
2	0% B	4.85±0.15	32.77±0.32	96.5±0.4	
3	0% B	3.02±0.13	4.28±0.32	92.2±0.1	
4	0% B	3.02±0.13	32.77±0.32	97.6±0.3	
5	1.05% B	2.98±0.06	4.32±0.30	61.0±0.1	
6	1.05% B	2.98±0.06	32.77±0.32	80.8±0.2	
7	1.62% B	2.98±0.05	4.32±0.30	57.6±0.2	
8	1.62% B	2.98±0.05	32.77±0.32	79.0±0.3	
9	Boral	7.13±0.11	32.77±0.32	67.2±0.1	
24	Al	6.25±0.01	1.05±0.29	107.2±0.1	
25	Al	6.25±0.01	32.77±0.32	107.7±0.5	
26	Zr-4	6.52±0.08	0.78±0.30	109.2±0.4	
27	Zr-4	6.52±0.08	32.77±0.32	108.6±0.4	]]

4.5. LEU-COMP-THERM-016 Results

The benchmark models for these experiments were created based on the generic MCNP input model provided in Appendix A.2 of LEU-COMP-THERM-016. All of the material composition atom density data used in the models was taken directly from the Tables 34, 35, 36 and 37 of LEU-COMP-THERM-016 for consistency with the internationally recognized experimental evaluation.

A total of twenty experiments were modeled. The system was full water reflected on all six sides by at least 12 inches of water. All calculations were performed with material and cross-section data representative of the system at 20°C. The Benchmark model k_{eff} was 1.000±0.0031 for these experiments.

Table 4-6 presents the results. For all twenty cases, the active fuel pin radius of 0.5588 cm and the square lattice pitch of 2.032 cm resulted in an effective (W/F) ratio of 3.209.

Table 4-6 - Benchmark Results for LEU-COMP-THERM-016

Case	Plate Type	Plate Thks. (mm)	Distance to Center Cluster (mm)	Cluster Separation (mm)	$K_{eff} \pm 1\sigma$
1	Steel 0%B	4.85±0.15	6.45±0.06	68.8±0.2	[[
2	Steel 0%B	4.85±0.15	27.32±0.5	76.4±0.4	
3	Steel 0%B	4.85±0.15	40.42±0.7	75.1±0.3	
4	Steel 0%B	3.02±0.13	6.45±0.06	74.2±0.2	
5	Steel 0%B	3.02±0.13	40.42±0.7	77.6±0.3	
6	Steel 0%B	3.02±0.13	6.45±0.06	104.4±0.3	
7	Steel 0%B	3.02±0.13	40.42±0.7	114.7±0.3	
8	Steel 1.05%B	2.98±0.06	6.45±0.06	75.6±0.2	
9	Steel 1.05%B	2.98±0.06	40.42±0.7	96.2±0.3	
10	Steel 1.62%B	2.98±0.05	6.45±0.06	73.6±0.3	
11	Steel 1.62%B	2.98±0.05	40.42±0.7	95.2±0.3	
12	Boral	7.13±0.11	6.45±0.06	63.3±0.5	
13	Boral	7.13±0.11	44.42±0.60	90.3±0.5	
14	Boral	7.13±0.11	6.45±0.06	50.5±0.3	
18	Copper	3.37±0.08	6.45±0.06	68.8±0.5	
28	Al	6.25±0.01	6.45±0.06	86.7±0.3	
29	Al	6.25±0.01	40.42±0.7	87.8±0.3	
30	Al	6.25±0.01	44.42±0.60	88.3±0.3	
31	Zircaloy	6.52±0.08	6.45±0.06	87.9±0.3	
32	Zircaloy	6.52±0.08	40.42±0.7	87.8±0.4	]]

4.6. LEU-COMP-THERM-034 Results

The benchmark models for these experiments were created based on the generic MCNP input model provided in Appendix A.2 of LEU-COMP-THERM-034. All of the material composition atom density data used in the models was taken directly from the Tables 13 and 14 of the LEU-COMP-THERM-034 for consistency with the internationally recognized experimental evaluation.

A total of fourteen experiments were modeled. The system was full water reflected on all six sides by at least 12 inches of water. All calculations were performed with material and cross-section data representative of the system at 20°C. The Benchmark model k_{eff} was 1.000 for these experiments. The uncertainty ranged from 0.0039 to 0.0048

Table 4-7 presents the results of the benchmark calculations. For all fourteen cases, the active fuel pin radius of 0.395 cm and the square lattice pitch of 1.60 cm resulted in an effective (W/F) ratio of 4.223.

Table 4-7 - Benchmark Results for LEU-COMP-THERM-034

Case	Canister	Water Gap (cm)	Critical Water Height (cm)	$K_{eff} \pm 1\sigma$
1	Borated Steel	0.6	34.33±0.06	[[
2	Borated Steel	1.0	36.54±0.06	
3	Borated Steel	2.0	41.40±0.08	
4	Borated Steel	3.0	47.15±0.07	
5	Borated Steel	4.0	53.87±0.07	
6	Borated Steel	5.0	62.86±0.08	
7	Borated Steel	6.0	70.73±0.06	
8	Borated Steel	7.0	80.66±0.06	
10	Boral	0.3	50.74±0.06	
11	Boral	0.5	53.01±0.06	
12	Boral	1.0	57.43±0.06	
13	Boral	1.5	66.15±0.06	
14	Boral	2.0	72.96±0.06	
15	Boral	2.5	84.15±0.07	]]

4.7. LEU-COMP-THERM-039 Results

The benchmark models for these experiments were created based on the information provided in Appendix A.2 of LEU-COMP-THERM-039. All of the material composition atom density data used in the models was taken directly from the Table 9 of the LEU-COMP-THERM-039 for consistency with the internationally recognized experimental evaluation.

A total of seventeen experiments were modeled. The system was full water reflected on all six sides by at least 12 inches of water. All calculations were performed with material and cross-section data representative of the system at 20°C. The Benchmark model k_{eff} was 1.000±0.0014 for these experiments.

Table 4-8 presents the results of the benchmark calculations. For all seventeen cases, the active fuel pin radius of 0.395 cm and the square lattice pitch of 1.26 cm were held constant. However, different combinations of rods were removed from the array resulting a variety of effective (W/F) ratios for the tests. The (W/F) ratios are given for each case in Table 4-8.

Table 4-8 - Benchmark Results for LEU-COMP-THERM-039

Case	# Rods	# Holes	Critical Water Height (cm)	W/F	$K_{eff} \pm 1\sigma$
1	459	25	81.36±0.07	2.415	[[
2	448	36	77.69±0.06	2.499	
3	420	64	73.05±0.06	2.732	
4	392	49	89.07±0.06	2.644	
5	320	121	84.37±0.06	3.464	
6	363	121	58.77±0.06	3.319	
7	459	25	69.71±0.06	2.415	
8	448	36	66.79±0.06	2.499	
9	448	36	64.47±0.06	2.499	
10	420	64	58.37±0.06	2.732	
11	459	25	81.34±0.06	2.415	
12	459	25	75.38±0.07	2.415	
13	459	25	72.52±0.06	2.415	
14	459	25	71.14±0.06	2.415	
15	459	25	69.88±0.06	2.415	
16	459	25	69.40±0.06	2.415	
17	459	25	68.75±0.06	2.415	]]

4.8. LEU-COMP-THERM-062 Results

The benchmark models for these experiments were created based on the generic MCNP input model provided in Appendix A.2 of LEU-COMP-THERM-062. All of the material composition atom density data used in the models was taken directly from the Tables 19, 20, 21, 22, 23 and 24 of the LEU-COMP-THERM-062 for consistency with the internationally recognized experimental evaluation.

A total of fifteen experiments were modeled. The system was full water reflected on all six sides by at least 12 inches of water. All calculations were performed with material and cross-section data representative of the system at 20°C. The Benchmark model k_{eff} was 1.000±0.0016 for these experiments.

Table 4-9 presents the results of the benchmark calculations. For all fifteen cases, the active fuel pin radius of 0.6251 cm and the square lattice pitch of 1.956 cm resulted in an effective (W/F) ratio of 2.116.

Table 4-9 - Benchmark Results for LEU-COMP-THERM-062

Case	Critical Water Height (cm)	Gap Width (cm)	Plate Thks. (cm)	Boron (wt.%)	$K_{eff} \pm 1\sigma$
1	80.89	0	N/A	N/A	[[
2	89.78	0	0.2910	0	
3	92.68	0	0.5820	0	
4	89.85	0.9779	0.5820	0	
5	86.42	1.9558	0.5820	0	
6	111.50	0	0.3114	0.67	
7	112.71	0	0.6228	0.67	
8	104.14	0.9779	0.3114	0.67	
9	98.74	0.9779	0.6228	0.67	
10	96.51	1.9558	0.3114	0.67	
11	92.31	1.9558	0.6228	0.67	
12	112.81	0	0.3097	0.98	
13	116.40	0	0.6194	0.98	
14	104.77	0.9779	0.6194	0.98	
15	95.55	1.9558	0.6194	0.98	]]

4.9. LEU-COMP-THERM-065 Results

The benchmark models for these experiments were created based on the generic MCNP input model provided in Appendix A.2 of LEU-COMP-THERM-065. All of the material composition atom density data used in the models was taken directly from the Tables 19, 20, 21, 22, 23 and 24 of the LEU-COMP-THERM-065 for consistency with the internationally recognized experimental evaluation.

A total of fifteen experiments were modeled. The system was full water reflected on all six sides by at least 12 inches of water. All calculations were performed with material and cross-section data representative of the system at 20°C. The Benchmark model k_{eff} ranged from 0.9994 to 1.0005 for these experiments. The uncertainty ranged from 0.0014 to 0.0017.

Table 4-10 presents the results of the benchmark calculations. For all seventeen cases, the active fuel pin radius of 0.6251 cm and the square lattice pitch of 1.956 cm resulted in an effective (W/F) ratio of 2.116.

Table 4-10 - Benchmark Results for LEU-COMP-THERM-065

Case	Crticial Water Level (cm)	Gap Width (cm)	Distance (cm)	Plate Thks. (cm)	Boron (wt.%)	$K_{eff} \pm 1\sigma$
1	50.62	N/A	2.9337	N/A	N/A	[[
2	61.56	0	2.9337	0.5820	0	
3	81.01	0	2.9337	0.6228	0.67	
4	84.44	0	2.9337	0.6194	0.98	
5	57.94	N/A	3.9116	N/A	N/A	
6	65.26	0	3.9116	0.2910	0	
7	64.20	0.9779	3.9116	0.2910	0	
8	68.98	0	3.9116	0.5820	0	
9	66.51	0.9779	3.9116	0.5820	0	
10	86.20	0	3.9116	0.3114	0.67	
11	78.18	0.9779	3.9116	0.3114	0.67	
12	88.73	0	3.9116	0.6228	0.67	
13	77.95	0.9779	3.9116	0.6228	0.67	
14	90.82	0	3.9116	0.3097	0.98	
15	80.22	0.9779	3.9116	0.3097	0.98	
16	93.02	0	3.9116	0.6194	0.98	
17	80.65	0.9779	3.9116	0.6194	0.98	]]

4.10. Jersey Central Criticals with and without Poison Curtains

[[

]]

Table 4-11 - Benchmark Results for Jersey Central Small Core Criticals

[[		
		]]

4.11. Small Core Criticals with Burnable Absorbers (KRITZ-75)

[[

]]

Table 4-12 - Benchmark Results for KRITZ-75 Small Core Criticals

[[				
				]]

4.12. NCA Step II & Step III Criticals

[[

]]

Table 4-13 - Benchmark Results for NCA Step II & Step III Criticals

[[						
						]]

4.13. NCA GNF1 Criticals

[[

]]

Table 4-14 - Benchmark Results for NCA GNF1 Criticals

[[									
									]]

[[

]]

[[

]]

Figure 4-1 – NCA GNF1 Experiments with 5 mm Aluminum Spacer

[[

]]

[[

]]

Figure 4-2 – [[ ]]

[[

]]

[[

]]

Figure 4-3 – Axial Gamma Scan Comparison for Rod A

[[

]]

[[

]]

Figure 4-4 – [[ ]]

[[

]]

Figure 4-5 – [[ ]]

[[

]]

[[

]]

Figure 4-6 – [[ ]]

[[

]]

[[

]]

[[

]]

Figure 4-7 – [[ ]]

[[

]]

[[

]]

Figure 4-8 – [[ ]]

[[

]]

[[

]]

Figure 4-9 – [[ ]]

[[

]]

[[

]]

Figure 4-10 – [[ ]]

[[

]]

[[

]]

Figure 4-11 – [[ ]]

[[

]]

5. Statistical Analysis of Results

5.1. MCNP01A Results as an Individual Population Sample

Figure 5-1 shows the results of a statistical analysis of all 190 benchmark eigenvalues treated as a single population sample with no correlation to any particular independent variable.

[[

]]

Figure 5-1.

MCNP01A Results Treated as a Single Population Sample

As can be seen from the results in Figure 5-1, the population sample has a mean value [[ ]]. If we state that the null hypothesis (H_o) is that the mean (μ) of the sample data is constant, then the alternative hypothesis (H_a) would be that the mean (μ) is not constant. [[

]]

In the following sections a sensitivity of the eigenvalue results will be performed to several independent correlation variables which are known to influence the reactivity of the critical systems under consideration. Examples of such variables would be effective water-to-fuel (W/F) ratio, absorber plate thickness and effective gadolinium rod wt% loading of the fuel pins. Sections 5.2 through 5.4 will consider these effects.

5.2. MCNP01A Eigenvalues Correlated to W/F Ratio

Figure 5-2 show the results of the MCNP01A eigenvalue calculations for all 190 experimental benchmark cases as a function of water-to-fuel (W/F) ratio for each experiment. The (W/F) ratio was chosen as the independent correlation variable since it is common to all experiments and affects the relative degree of moderation within the lattice.

[[

]]

Figure 5-2.

MCNP01A Resutls as a Function of W/F Ratio

[[

]]

5.3. MCNP01A Eigenvalues for Absorber Plate Sytems

An alternative way of evaluating the results of the MCNP01A benchmark calculations is to group only those experiments that contained absorber plates between array clusters (to simulate storage rack conditions). These experiments include LEU-COMP-THERM-009, 016, 034, 062 and 065 (seventy-nine experiments in all). A normality test of this data is shown in Figure 5-3 below.

[[

]]

Figure 5-3. Results for Absorber Plate Criticals Only

[[

]]

[[

]]

Figure 5-4

Results for Absorber Plate Criticals as a Function of W/F Ratio

[[

]]

[[

]]

[[

]]

Figure 5-5.

Results for Absorber Plate Criticals as a Function of Plate Thickness

[[

]]

5.4. MCNP01A Eigenvalues for Gadolinium Systems

[[

]]

[[

]]

Figure 5-6.

Results for NCA Step II, Step III and GNF1 Criticals with Gd_2O_3

[[

]]

[[

]]

Figure 5-7.

Results Correlated to the Number of Gd Rods in Each Test Zone Lattice

[[

]]

[[

]]

Figure 5-8.

Results Correlated to the Number of Gd Rods in Each Test Zone Lattice

[[

]]

6. Bias and Bias Uncertainty

In order to account for the uncertainty in the experimental values (Reference 16), the weighted sample mean and standard deviation were calculated using the following equations:

$$B = Measured\ \ K_{eff} - Calculated\ (MCNP01A)\ \ K_{eff} \qquad \textbf{Equation 1}$$

$$\overline{B} = \frac{\sum_{i=1}^{n} \frac{B_i}{\sigma_i^2}}{\sum_{i=1}^{n} \frac{1}{\sigma_i^2}} \qquad \textbf{Equation 2}$$

$$S_P = \sqrt{s^2 + \overline{\sigma}^2} \qquad \textbf{Equation 3}$$

$$\overline{\sigma}^2 = \frac{n}{\sum_{i=1}^{n} \frac{1}{\sigma_i^2}} \qquad \textbf{Equation 4}$$

$$s^2 = \frac{\left(\frac{1}{n-1}\right)\sum_{i=1}^{n} \frac{1}{\sigma_i^2}\left(B_i - \overline{B}\right)^2}{\frac{1}{n}\sum_{i=1}^{n} \frac{1}{\sigma_i^2}} \qquad \textbf{Equation 5}$$

Where:

$\overline{B}$ = Average weighted bias in K_{eff}

σ_i = Uncertainty in bias Bi

S_P = Pooled standard deviation

s^2 = Variance about the mean

$\overline{\sigma}^2$ = Average total variance

n = number of data points (=190)

Using the average weighted bias and pooled standard deviation; the upper one-sided 95/95-tolerance limit (Reference 17) and the bias uncertainty were calculated for use in criticality calculations. Table 6-1 summarizes the results of these calculations.

Table 6-1 - Bias and Bias Uncertainty Results for MCNP01A with ENDF/B-V

[[	
	]]

*Bias=Benchmark-MCNP01A

7. Conclusions/Recommendations

The 190 experimental benchmark data set studied in this report adequately simulates the lattice physics characteristics of typical BWR fuel lattices. The experimental range of W/F ratio extends from ~0.8 up to 4.2 for low-enriched UO2 pin lattice in water systems. All of the experiments considered are judged to be acceptable as benchmark experiments either by virtue of their inclusion in Reference 3 (previously

accepted by the International Benchmark Evaluation Group) or by their historical use within the BWR nuclear fuels community.

The data is judged to be acceptable for the determination of code and cross-section data set bias and bias uncertainty for application to spent fuel storage rack criticality safety analysis as well as for the purposes of lattice physics benchmaking of other transport method codes. [[

]]

The recommended bias and bias uncertainty to be used with criticality analyses are shown in Table 7-1.

Table7-1: Recommended Bias and Bias Uncertainty in Criticality Analyses for MCNP01A with ENDF/B-V

[[	
	]]

8. References

1. MCNP4A – "Monte Carlo N-Particle Code System", Los Alamos Nat. Lab., Distributed by RSIC, CCC-200, December 1993.
2. MCNP01A; General Electric version of Los Alamos National Laboratory code, MCNP4A – General Monte Carlo N-Particle Transport Code, DRF J11-02538, March, 1995.
3. International Criticality Safety Benchmark Evaluation Project (ICSBEP), LEU-COMP-THERM-001 – 063, Benchmark Experiments, September 2005.
4. S.R. Bierman, E.D. Clayton and B.M. Durst, "Critical Separation Between Subcritical Clusters of 2.35 wt.% Enriched UO_2 Rods in Water with Fixed Neutron Poisons", PNL-2438, Battelle Pacific Northwest Laboratories, Richland, Washington, October 1977.
5. S.R. Bierman and E.D. Clayton, "Criticaltiy Experiments with Subcritical Clusters of 2.35 wt.% and 4.31 wt.% Enriched UO_2 Rods in Water at a Water-to-Fuel Volume Ratio of 1.6", NUREG/CR-1547, PNL-3314, Battelle Pacific Northwest Laboratories, Richland, Washington, July 1980.
6. S.R. Bierman, B.M. Durst and E.D. Clayton, "Critical Separation Between Subcritical Clusters of 4.29 wt.% ^{235}U Enriched UO_2 Rods in Water with Fixed Neutron Poisons", NUREG/CR-0073, Battelle Pacific Northwest Laboratories, Richland, Washington, May 1978.
7. Harumichi Tsuruta, Iwao Kobayashi, Takenori Suzaki, Akio Ohno, Kiyonobu Murakami and Syojiro Matsuura, "Critical Sized of Light Water Moderated UO_2 and PuO_2-UO_2 Lattices", JAERI-1254, 1978.
8. J.C. Manaranche, D. Mangin, L. Maubert, G. Colomb, G. Poullot, "Experimental Studies of LWR Fuel Rods in Various Configurations", Rappaport DSN, 399/80, December 1980.

9. J.C. Manaranche, D. Mangin, L. Maubert, G. Colomb, G. Poullot, "Critical Experiments with Lattices of 4.75 wt.% U-235 Enriched UO_2 Rods in Water", Nucl. Sci. & Eng., Vol. 71, pp. 143-163, 1979.

10. Yoshinori Miyoshi, Ken Nakajima, Masanori Akia, Akio Ohno, Iwao Kobayashi, Shigeaki Aoki, Masayuki Harada, Chirio Hondo and Ichiro Deguchi, "Reactivity Effects of Borated Steel Plate in Single and Coupled Cores Composed of Low-Enriched UO_2 Rods", Journal of Nuclear Science and Technology, Vol. [31]4, pp. 335-348, 1994.

11. C.L. Martin, "Lattice Physics Methods Verification", GE Nuclear Energy, NEDO-20939, Class I, June 1976.

12. S. Sitaraman,"MCNP: Light Water Reactor Critical Benchmarks", GE Nuclear Energy, NEDO-32028, Class I, March 1992.

13. Persson, R. and Johansson, E., "KRITZ BA-75: Critical High Temperature Experiments on BWR Assemblies with Burnable Absorbers – August-December 1975," AB Atomenergi Sweden, AE-RF-76-4154, February 1976 (English Translation October 1976).

14. Y. Karino, "MCNP:TGBLA03/DIF3D:TGBLA06V/DIF3D Benchmarking of Toshiba's NCA Critical Facility", GE Nuclear Energy, NEDC-32609P, Class III, May 1996.

15. SCO-01-2047, "2001 Critical Examination of PLR/Corner Gad", Toshiba Electric Power Corporation, December 2001.

16. NUREG/CR-6698 "Guide For Validation of Nuclear Criticality Safety Calculational Methodology", Science Applications International Corporation, January 2001.

17. NIST/SEMATECH e-Handbook of Statistical Methods,

http://www.itl.nist.gov/div898/handbook/prc/section2/prc263.htm, 2006

Appendix: MCNP01A Benchmark Results

#	Experiment	Expt. #	Benchmark Eigenvalue	Experimental Uncertainty	MCNP01A	MCNP01A Uncertainty	Bias	Bias Uncertainty
1	LEU-COMP-THERM-001	1	0.9998	0.0031	[[			
2	LEU-COMP-THERM-001	2	0.9998	0.0031				
3	LEU-COMP-THERM-001	3	0.9998	0.0031				
4	LEU-COMP-THERM-001	4	0.9998	0.0031				
5	LEU-COMP-THERM-001	5	0.9998	0.0031				
6	LEU-COMP-THERM-001	6	0.9998	0.0031				
7	LEU-COMP-THERM-001	7	0.9998	0.0031				
8	LEU-COMP-THERM-001	8	0.9998	0.0031				
9	LEU-COMP-THERM-002	1	0.9997	0.002				
10	LEU-COMP-THERM-002	2	0.9997	0.002				
11	LEU-COMP-THERM-002	3	0.9997	0.002				
12	LEU-COMP-THERM-002	4	0.9997	0.002				
13	LEU-COMP-THERM-002	5	0.9997	0.002				
14	LEU-COMP-THERM-006	1	1	0.002				
15	LEU-COMP-THERM-006	2	1	0.002				
16	LEU-COMP-THERM-006	3	1	0.002				
17	LEU-COMP-THERM-006	4	1	0.002				
18	LEU-COMP-THERM-006	5	1	0.002				
19	LEU-COMP-THERM-006	6	1	0.002				
20	LEU-COMP-THERM-006	7	1	0.002				
21	LEU-COMP-THERM-006	8	1	0.002				
22	LEU-COMP-THERM-006	9	1	0.002				
23	LEU-COMP-THERM-006	10	1	0.002				
24	LEU-COMP-THERM-006	11	1	0.002				
25	LEU-COMP-THERM-006	12	1	0.002				

26	LEU-COMP-THERM-006	13	1	0.002				
27	LEU-COMP-THERM-006	14	1	0.002				
28	LEU-COMP-THERM-006	15	1	0.002				
29	LEU-COMP-THERM-006	16	1	0.002				
30	LEU-COMP-THERM-006	17	1	0.002				
31	LEU-COMP-THERM-006	18	1	0.002				
32	LEU-COMP-THERM-009	1	1	0.0021				
33	LEU-COMP-THERM-009	2	1	0.0021				
34	LEU-COMP-THERM-009	3	1	0.0021				
35	LEU-COMP-THERM-009	4	1	0.0021				
36	LEU-COMP-THERM-009	5	1	0.0021				
37	LEU-COMP-THERM-009	6	1	0.0021				
38	LEU-COMP-THERM-009	7	1	0.0021				
39	LEU-COMP-THERM-009	8	1	0.0021				
40	LEU-COMP-THERM-009	9	1	0.0021				
41	LEU-COMP-THERM-009	24	1	0.0021				
42	LEU-COMP-THERM-009	25	1	0.0021				
43	LEU-COMP-THERM-009	26	1	0.0021				
44	LEU-COMP-THERM-009	27	1	0.0021				
45	LEU-COMP-THERM-016	1	1	0.0031				
46	LEU-COMP-THERM-016	2	1	0.0031				
47	LEU-COMP-THERM-016	3	1	0.0031				
48	LEU-COMP-THERM-016	4	1	0.0031				
49	LEU-COMP-THERM-016	5	1	0.0031				
50	LEU-COMP-THERM-016	6	1	0.0031				
51	LEU-COMP-THERM-016	7	1	0.0031				
52	LEU-COMP-THERM-016	8	1	0.0031				
53	LEU-COMP-THERM-016	9	1	0.0031				
54	LEU-COMP-THERM-016	10	1	0.0031				

55	LEU-COMP-THERM-016	11	1	0.0031				
56	LEU-COMP-THERM-016	12	1	0.0031				
57	LEU-COMP-THERM-016	13	1	0.0031				
58	LEU-COMP-THERM-016	14	1	0.0031				
59	LEU-COMP-THERM-016	18	1	0.0031				
60	LEU-COMP-THERM-016	28	1	0.0031				
61	LEU-COMP-THERM-016	29	1	0.0031				
62	LEU-COMP-THERM-016	30	1	0.0031				
63	LEU-COMP-THERM-016	31	1	0.0031				
64	LEU-COMP-THERM-016	32	1	0.0031				
65	LEU-COMP-THERM-034	1	1	0.0047				
66	LEU-COMP-THERM-034	2	1	0.0047				
67	LEU-COMP-THERM-034	3	1	0.0039				
68	LEU-COMP-THERM-034	4	1	0.0039				
69	LEU-COMP-THERM-034	5	1	0.0039				
70	LEU-COMP-THERM-034	6	1	0.0039				
71	LEU-COMP-THERM-034	7	1	0.0039				
72	LEU-COMP-THERM-034	8	1	0.0039				
73	LEU-COMP-THERM-034	10	1	0.0048				
74	LEU-COMP-THERM-034	11	1	0.0048				
75	LEU-COMP-THERM-034	12	1	0.0048				
76	LEU-COMP-THERM-034	13	1	0.0048				
77	LEU-COMP-THERM-034	14	1	0.0043				
78	LEU-COMP-THERM-034	15	1	0.0043				
79	LEU-COMP-THERM-039	1	1	0.0014				
80	LEU-COMP-THERM-039	2	1	0.0014				
81	LEU-COMP-THERM-039	3	1	0.0014				
82	LEU-COMP-THERM-039	4	1	0.0014				
83	LEU-COMP-THERM-039	5	1	0.0014				

84	LEU-COMP-THERM-039	6	1	0.0014				
85	LEU-COMP-THERM-039	7	1	0.0014				
86	LEU-COMP-THERM-039	8	1	0.0014				
87	LEU-COMP-THERM-039	9	1	0.0014				
88	LEU-COMP-THERM-039	10	1	0.0014				
89	LEU-COMP-THERM-039	11	1	0.0014				
90	LEU-COMP-THERM-039	12	1	0.0014				
91	LEU-COMP-THERM-039	13	1	0.0014				
92	LEU-COMP-THERM-039	14	1	0.0014				
93	LEU-COMP-THERM-039	15	1	0.0014				
94	LEU-COMP-THERM-039	16	1	0.0014				
95	LEU-COMP-THERM-039	17	1	0.0014				
96	LEU-COMP-THERM-062	1	1	0.0016				
97	LEU-COMP-THERM-062	2	1	0.0016				
98	LEU-COMP-THERM-062	3	1	0.0016				
99	LEU-COMP-THERM-062	4	1	0.0016				
100	LEU-COMP-THERM-062	5	1	0.0016				
101	LEU-COMP-THERM-062	6	1	0.0016				
102	LEU-COMP-THERM-062	7	1	0.0016				
103	LEU-COMP-THERM-062	8	1	0.0016				
104	LEU-COMP-THERM-062	9	1	0.0016				
105	LEU-COMP-THERM-062	10	1	0.0016				
106	LEU-COMP-THERM-062	11	1	0.0016				
107	LEU-COMP-THERM-062	12	1	0.0016				
108	LEU-COMP-THERM-062	13	1	0.0016				
109	LEU-COMP-THERM-062	14	1	0.0016				
110	LEU-COMP-THERM-062	15	1	0.0016				
111	LEU-COMP-THERM-065	1	1	0.0014				
112	LEU-COMP-THERM-065	2	0.9999	0.0014				

113	LEU-COMP-THERM-065	3	0.9996	0.0015				
114	LEU-COMP-THERM-065	4	0.9997	0.0015				
115	LEU-COMP-THERM-065	5	1	0.0014				
116	LEU-COMP-THERM-065	6	0.9998	0.0014				
117	LEU-COMP-THERM-065	7	0.9991	0.0014				
118	LEU-COMP-THERM-065	8	1	0.0016				
119	LEU-COMP-THERM-065	9	1.0001	0.0015				
120	LEU-COMP-THERM-065	10	1.0002	0.0016				
121	LEU-COMP-THERM-065	11	1.0005	0.0016				
122	LEU-COMP-THERM-065	12	1	0.0017				
123	LEU-COMP-THERM-065	13	1.0001	0.0016				
124	LEU-COMP-THERM-065	14	1.0003	0.0016				
125	LEU-COMP-THERM-065	15	0.9994	0.0016				
126	LEU-COMP-THERM-065	16	0.9998	0.0017				
127	LEU-COMP-THERM-065	17	1.0003	0.0016				]]
128	[[							
129								
130								
131								
132								
133								
134								
135								
136								
137								
138								
139								
140								
141								

142								
143								
144								
145								
146								
147								
148								
149								
150								
151								
152								
153								
154								
155								
156								
157								
158								
159								
160								
161								
162								
163								
164								
165								
166								
167								
168								
169								
170								

171								
172								
173								
174								
175								
176								
177								
178								
179								
180								
181								
182								
183								
184								
185								
186								
187								
188								
189								
190								]]

Bias=Benchmark-MCNP01A